Aus der Klinik für Allgemeine-, Viszerale- und Transplantationschirurgie

Klinik der Ludwig-Maximilians-Universität München

Tigecycline affects RAC1 and OXPHOS and shows antitumor effect in hepatocellular carcinoma

Dissertation

zum Erwerb des Doktorgrades der Medizin

an der Medizinischen Fakultät der

Ludwig-Maximilians-Universität München

vorgelegt von

Haochen Yu

aus

ChongQing

Jahr

2022

Mit Genehmigung der Medizinischen Fakultät der

Ludwig-Maximilians-Universität zu München

Erster Gutachter:	Prof. Dr. Alexandr Bazhin
Zweiter Gutachter:	apl. Prof. Dr. Michael Berger
Dritter Gutachter:	apl. Prof. Dr. Enrico De Toni
ggf. weitere Gutachter:	
Mitbetreuung durch den promovierten Mitarbeiter:	
Dekan:	Prof. Dr. med. Thomas Gudermann
Tag der mündlichen Prüfung:	22.07.2022

Table of content

Zusammenfassung (Deutsch):

Hintergrund: Das hepatozelluläre Karzinom (HCC) hat eine hohe Morbiditäts- und Mortalitätsrate, jedoch sind die entsprechenden Behandlungsmöglichkeiten limitiert. Mit dem Fortschreiten der Antibiotikaforschung wurde auch die tumorhemmende Wirkung von Antibiotika entdeckt. Unter anderem zeigt auch das Glycylcyclin Tigecyclin antitumorale Wirkung und ist Gegenstand dieser Studie, um die Wirkung gegen Leberzellkarzinome zu untersuchen und dessen Mechanismus zu erforschen.

Methoden: HCC-Zellen und Hepatozyten wurden mit unterschiedlichen Konzentrationen von Tigecyclin behandelt. MTT und CV wurden verwendet, um die posttherapeutische metabolische Aktivität der Zellen zu messen und die mittlere inhibitorische Konzentration (IC_{50}) zu berechnen. Sphere Formation Assays wurden benutzt, um Veränderungen der Stammzellen festzustellen. Des Weiteren wurden Wundheilungsassays und Transwell-Assays verwendet, um Veränderungen der Zellmigrations- und der Invasionsfähigkeit zu analysieren. Zudem wurden bioinformatische Analysen zur Identifizierung potenzieller Ziele von RAC1 eingesetzt. Western blot und RT-PCR wurden zum Nachweis der Expression relevanter Marker durchgeführt. DCHA wurde angewendet, um die Produktion reaktiver Sauerstoffspezies nach der Behandlung mit Tigecyclin nachzuweisen. Darüber hinaus wurde auch die Durchflusszytometrie hinzugezogen, um Veränderungen in verschiedenen Zellzyklen nach der Tigecyclin-Behandlung zu erkennen. Die Seahorse-Analyse wurde eingesetzt, um Veränderungen in der mitochondrialen Funktion nach der Zellbehandlung festzustellen.

Ergebnisse: Nach der Tigecyclin-Behandlung von HCC-Zellen und normalen Hepatozyten THLE-2 war die Lebensfähigkeit aller Zellen reduziert. Die Empfindlichkeit von HCC-Zellen gegenüber Tigecyclin war höher als die von THLE-2. Tigecyclin hemmte sowohl die Migration als auch die Invasion von HCC-Zellen. HCC-Zellen zeigten nach der Behandlung mit Tigecyclin

eine erhöhte Expression von RAC1, eine verringerte ROS-Produktion, eine veränderte Funktion der Mitochondrien und eine Verlangsamung der S-Phase des Zellzyklus. Die Inhibition von HCC-Zellen wird verstärkt, wenn Tigecyclin in Kombination mit Everolimus eingesetzt wird.

Schlußfolgerung: Unsere Studie zeigte erstmals die hemmende Wirkung von Tigecyclin auf HCC. Die Hemmung von RAC1, der Stillstand des Zellzyklus, die Verringerung von ROS und die mitochondriale oxidative Phosphorylierung könnten an diesem Prozess beteiligt sein. Vor allem aber haben wir festgestellt, dass Tigecyclin normale Hepatozyten nur begrenzt schädigt. Unsere Ergebnisse bieten mehr Möglichkeiten für den klinischen Einsatz von Tigecyclin bei HCC.

Abstract (English):

Background: Currently, hepatocellular carcinoma (HCC) has a high morbidity and mortality rate and corresponding treatment options are limited. Liver transplantation is highly limited by organ supply and liver resection is limited by high recurrence rates and there are no adjuvant therapy options to date. As antibiotic research progressed, antitumor effects of antibiotics were discovered. Therefore, we chose Tigecycline, a glycylcycline antibiotic, as the subject of our study to investigate the anti-HCC effects and to explore its mechanism to provide a perioperative antitumor therapy option.

Methods: HCC cells and hepatocytes were treated with different concentrations of Tigecycline. MTT and CV were used to assay their cell viability and to calculate IC_{50}. Sphere formation assays measured changes in cell stemness. To assess changes in cell migration and invasion capabilities, wound healing and transwell assays are used. RAC1 was identified as a possible target for Tigecycline by bioinformatics analysis. The expression of key markers was detected using Western blot and RT-PCR. DCHA was utilized to measure reactive oxygen species generation during Tigecycline therapy. FACS was used to detect alterations in cell cycle following Tigecycline treatment and changes in mitochondrial function were detected via seahorse analysis.

Results: After Tigecycline treatment of HCC cells the viability was reduced significantly. The sensitivity of HCC cells to Tigecycline was higher than that of immortalized normal hepatocytes THLE-2. Tigecycline inhibited both migration and invasion of HCC cells. HCC or hepatocytes cells showed increased expression of RAC1, decreased ROS production, reduced mitochondrial function and arrested in S-phase of the cell cycle after Tigecycline treatment. The inhibition of HCC cells is enhanced when Tigecycline is used in combination with Everolimus.

Conclusion： Our study firstly revealed the inhibitory effect of Tigecycline on HCC. Inhibition of RAC1, cell cycle arrest, reduction of ROS and mitochondrial oxidative phosphorylation may all be involved in the process. Most importantly, we also studied the effects of Tigecycline on normal hepatocytes and found that it caused limited damage to normal hepatocytes. Our findings provide more possibilities for the clinical use of Tigecycline in HCC.

List of figures

List of abbreviations

ATCC	American Type Culture Collection
APS	Ammonium persulfate
BCA	Bicinchoninic Acid
BEGM	Bronchial Epithelial Cell Growth Medium
bFGF	Basic Fibroblast Growth Factor
BSA	Bovine Serum Albumin
CML	Chronic Myeloid Leukemia
CTD	Comparative Toxicogenomics Database
CV	Crystal Violet
DCFH-DA	2',7'-Dichlorofluorescein Diacetate
DMSO	Dimethylsulfoxid
ECL	Enhanced chemiluminescence
EGF	Epidermal Growth Factor
ERK1	Extracellular Signal-Related Kinase 1
ERK2	Extracellular Signal-Related Kinase 2
FACS	Fluorescence-activated cell sorting
FBS	Fetal Bovine Serum
GIFtS	Genecards Inferred Functionality Score
GEFs	Guanine Nucleotide Exchange Factors
HBV	Hepatitis B Virus
HCC	Hepatocellular Carcinoma
HCV	Hepatitis C Virus
HNSCC	Head-And-Neck Squamous Cell Cancer
IC_{50}	Half Maximal Inhibitory Concentration
IVR	Ivermectin (IVR)
KEGG	Kyoto Encyclopedia of Genes And Genomes
mtRNA	Mitochondrial DNA
MDR	Multidrug resistance

MON	Monensin
NSCLC	Nonsmall Cell Lung Cancer
nucRNA	Nuclear DNA
PBS	Phosphate Buffered Saline
PFA	Paraformaldehyde
RAC1	Rac Family Small Gtpase 1
ROS	Reactive Oxygen Species
RTKs	Receptor Tyrosine Kinases
RT-PCR	Reverse Transcription‐Polymerase Chain Reaction
SD	Standard Deviation
SDS	Sodium dodecyl sulfate
SFA	Sphere Formation Assay
siRNA	Small Interfering RNA
SAL	Salinomycin
TBS	Tris-Buffered Saline
Tige	Tigecycline
TNTs	Tunneling Nanotubes

1. Introduction

The liver, as the biggest organ in the body, has a rich circulatory system, received blood mainly from hepatic artery and the portal vein. Therefore, the liver is exposed to a large proportion of microbial products through the intestine. As a result, the liver is an important metabolic and detoxification organ. Millions of people worldwide are affected by liver disease. In most developed areas such as Europe and the United States, the incidence of viral hepatitis is waning due to advances in disease prevention, diagnosis, and treatment. At the same time, the massive expansion of vaccines against hepatitis B viruses in many countries, like China, has also led to a dramatic decline in new cases. Conversely, as living standards improve, the incidence of metabolic liver disease (non-alcoholic fatty liver disease and alcohol-related liver disease) will increase, finally leading to more cases of advanced-stage liver disease (liver failure, cirrhosis and liver cancer). And of all advanced liver diseases, liver cancer is undoubtedly the worst outcome for patients.

1.1 Liver cancer and hepatocellular carcinoma

1.1.1 The global epidemiological statistics of liver cancer

According to the latest data, liver cancer is the sixth most prevalent cancer type globally, and it is even the second or third largest cause of cancer-related fatalities. Especially in male, the cancer mortality rate is the second highest [1-3]. The 5-year survival of liver cancer is 18% [4]. The incidence and mortality rates of liver cancer also vary greatly between genders. In most regions of the world, the incidence and mortality rates are two to three times higher among men than in women. According to the World Health Organization 2020 report, among the most common types of cancer in 185 countries of the world, liver cancer is the most common in Mongolia with by far the highest incidence and mortality rates worldwide (93.7 and 75.4, respectively) [1].

The overall burden from liver cancer is most pronounced in transitioning countries; rates are highest in Eastern Asia, South-Eastern Asia, Northern Africa, and Micronesia (Fig. 1).

Different risk factors may lead to different types of liver cancer and have different trends. Primary liver cancer can be broadly subdivided into hepatocellular carcinoma (HCC) (typically 75-85% of all liver cancer cases) and intrahepatic cholangiocarcinoma (ICC) (approximately 10-15%), and others, more rare types [5]. ICC is associated with primary sclerosing cholangitis fibrous polycystic liver disease, parasitic infections, and intrahepatic bile duct stones [6]. As the most common form of liver cancer, HCC's epidemiological data are consistent with liver cancer.

HCC has several major causative risks. These factors include mainly long-term infection with hepatitis B and C viruses (HBV, HCV), obesity, smoking, long-term consumption of aflatoxin-contaminated food, diabetes and high alcohol intake [7]. Interestingly, the incidence in high-risk countries (e.g., China, Philippines, Thailand, etc.) has been declining for a long time [8], but in contrast the incidence in some low-risk countries such as Europe, South America, and Australia/New Zealand has been steadily increasing in recent years [9]. Declining prevalence of aflatoxin infection and exposure in high-risk areas like Eastern Asia may contribute to the declining incidence of HCC in these areas[10]. It is hypothesized that the continued increase in morbidity in low-risk areas is associated with an increased incidence of obesity and metabolic diseases such as diabetes. These new cases counterbalance the improvements obtained by lowering HBV and HCV prevalence [11, 12]. Fortunately, the incidence and mortality rates of liver cancer in adolescents and young adults aged 15 to 39 years are much lower, probably due to the long time it takes from precancerous lesions to tumor formation and the short time they are exposed to risk factors [13].

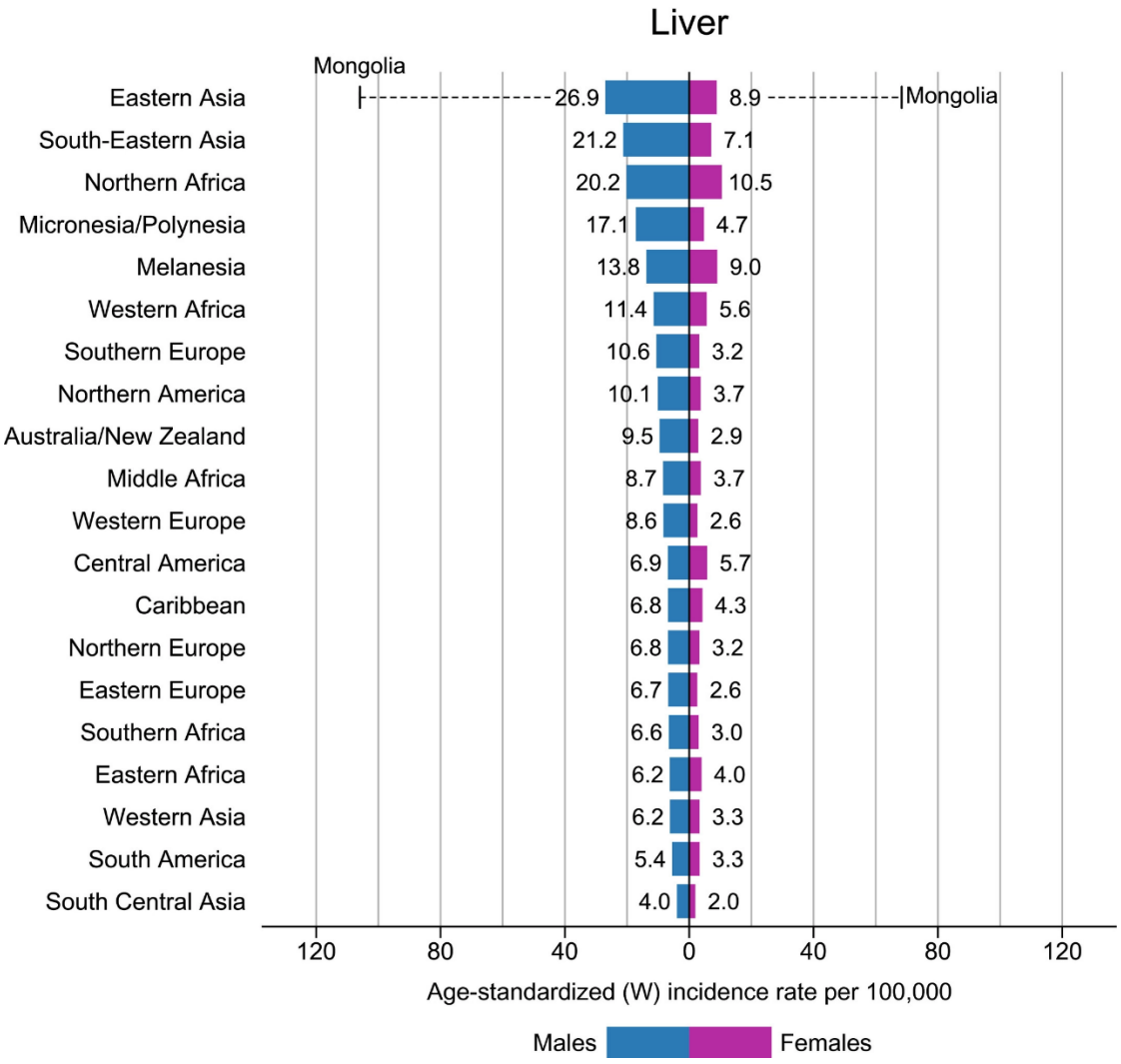

Figure 1: Region-Specific Incidence Age-Standardized Rates by Sex for Liver Cancer in 2020.

Rates are shown in descending order of the world (W) age-standardized rate among men, and the highest national rates among men and women are superimposed. Data from: GLOBOCAN 2020 (https://acsjournals.onlinelibrary.wiley.com/cms/asset/1f16ffd6-9a97-436d-b8ec45c54c231db6/caac21660-fig-0013-m.jpg).

1.1.2 Options for the treatment of hepatocellular carcinoma

Surgical removal, liver transplantation, local treatment, chemoembolization, and systemic chemotherapy are the five primary clinical therapeutic options for HCC [14].

With improvements in bleeding control, anesthesia techniques, perioperative care, surgical equipment, and an all-around understanding of liver anatomy, the prognosis for patients after liver resection is getting better [15]. It also allows many patients with tumors previously considered unsuitable for surgical resection to have the opportunity to undergo surgery. Depending on the size and location of the tumor in the liver, there are several types of curative liver resections including segmental resection, left or right hepatectomy, and extended left or right hepatectomy [16]. The application of new minimally invasive liver resections has increased in recent years with the development of minimally invasive techniques, laparoscopic techniques, and surgical robotics, and some articles suggest that this may be benefiting from improved short-term outcomes [17], but others suggest that the long-term outcomes of these new techniques need further validation [18, 19].

Liver transplantation is the most favorable treatment option for HCC patients. Liver transplantation achieves 5-year recurrence rates of 15%, whereas liver resection shows recurrence rates of more than 70% [20]. However, liver transplantation is limited especially in countries with limited organ supply. Liver transplantation is therefore mainly performed in patients fulfilling the Milan criteria. The Milan criteria include individuals who do not have macrovascular invasion or extrahepatic dissemination, as well as nodule size limitations of a single nodule less than or equal to 5 cm or no more than three nodules not exceeding 3 cm [21].

The Barcelona Clinic Liver Cancer (BCLC) staging system (Figure 2), remains the most widely used method for the systematic management of HCC patients in clinical practice to the current time. This recommendation states that surgical therapy is mostly determined by the patient's functional condition, underlying liver disease, and tumor size [22]. According to reports, only 30% of HCC patients are surgical candidates (liver resection and liver transplantation) [23].

Due to these limitations, resection needs to be performed and there is a need of improving recurrence rates after resection. One way of improving recurrence rates after resection is to establish new adjuvant therapy options. To date, there are no adjuvant therapy options established. In chemotherapy and systemic therapy, more than 100 randomized clinical trials have been reported testing chemotherapy or other types of systemic therapy for HCC, but only one drug, Sorafenib, has been shown to have a survival advantage [24-26]. Therefore, Sorafenib remains the first-line treatment option for HCC. Sorafenib, a first-line systemic treatment, is appropriate for patients in the C stage (BCLC standard) with maintained liver function, an ECOG-PS score of 1 to 2, and macrovascular invasion or extrahepatic dissemination [24] did not show any benefit when used as an adjuvant therapy option[27].

In addition, a similar drug, cabozantinib, is being tested as a second-line therapy after initial positive results in clinical studies [28]. Several clinical trials have found benefits of radiofrequency ablation for patients with early-stage HCC [14, 29, 30]. Five-years survival rates after radiofrequency ablation averages 60% [31]. However, for terminal stage patients, symptomatic treatment and end-of-life care are the only things we can do to alleviate their suffering.

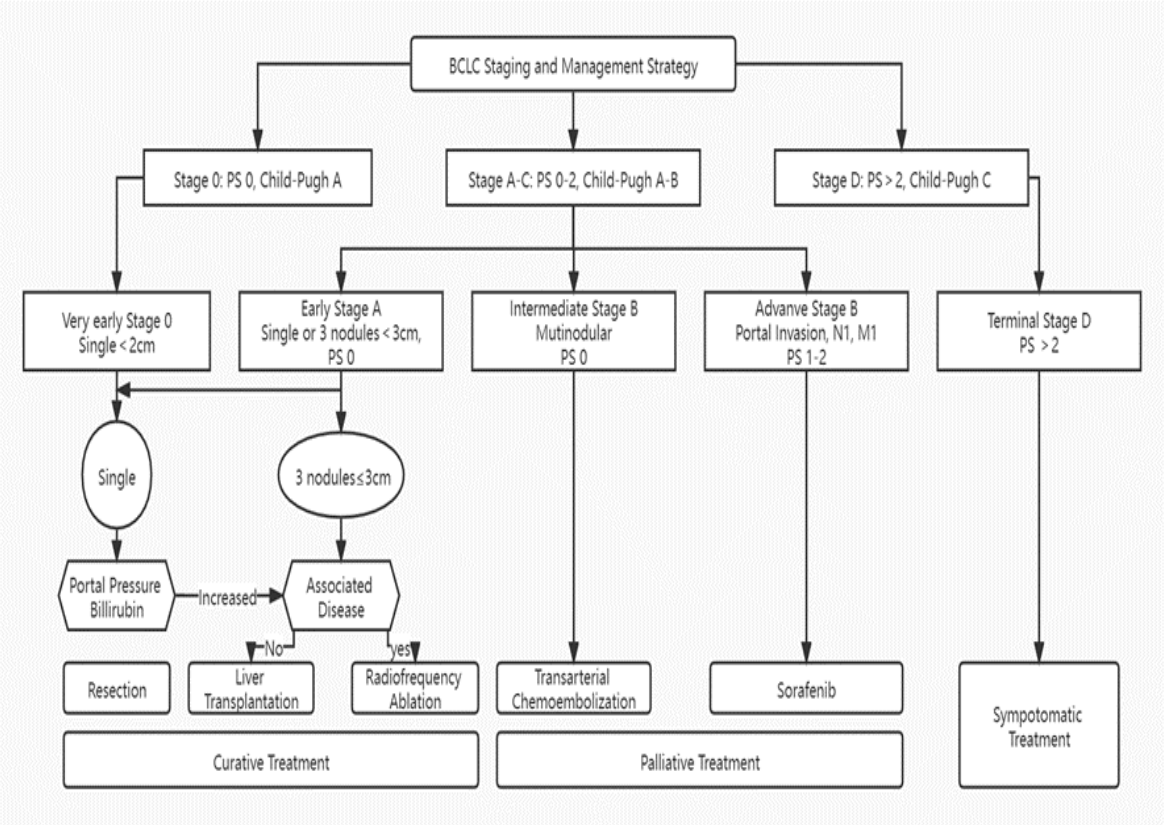

Figure 2. BCLC Staging and Treatment Strategy Flow Chart, modified from [22] (PS, performance status)

1.1.3 Classification of HCC based on molecular characteristics

Molecular classification of tumors is particularly important for the precision treatment of tumors. If the molecular characteristics of a tumor can be clarified, the development of relevant inhibitors or activators for the characteristics of these molecules is the main method of new tumor drug development. Among all tumors, the best-known molecular classification would be in the breast cancer. Based on the expression of ER, PR and HER2 genes breast cancer can be classified into Luminal A, Luminal B, HER2 and triple negative breast cancer (TNBC) [32]. The different treatment approaches for different subtypes have greatly improved the overall survival rate of breast cancer patients. Molecular subtypes of HCC have been identified by high-throughput sequencing. These molecular subtypes are distinguished by unique oncogene signaling pathways and recurrent mutations [33]. Even

though these molecular subtypes of HCC do not currently directly affect clinicians' diagnosis and decision making, correlations between these subtypes, pathological and clinical features (eg, clinical test results, risk factors, survival time, etc.) have been identified and are increasingly valued.

Unsupervised clustering of gene expression classified HCC into two major subtypes [34, 35]. Taking into account the clinicopathological features, pathogenic factors, and patient prognosis, HCC can be broadly classified into proliferation and non-proliferation subtypes, each subtype has its own unique molecular expression profile [35].

The proliferation subtype of HCC cells is mainly the progenitor-like, with a small percentage of hepatocyte-like [35]. The proliferation subtype of HCC was also shown to be mainly enriched in the proliferation pathway of tumor cells in the results of signaling pathways enrichment analysis. The pathway of insulin-like growth factor [36], mTOR [37], RAS [38], stem cell features [39] and the NOTCH [40] have all been found to be associated with the proliferation subtype. Thus, proliferation has a high degree of heterogeneity. Epigenetic studies have found that DNA methylation, microRNA expression patterns are associated with proliferative subtypes [41].

The nonproliferation subtype of HCC has a different molecular profile compared proliferation, in addition to better clinical symptoms and patient outcomes than proliferative subtypes. HCC of the nonproliferation subclass keep part hepatocyte-like characteristics; a subset includes activation of the canonical Wnt signaling pathway, mostly through mutations in CTNNB1 [35]. Also, canonical WNT signaling is considerably enriched in this class, as indicated by upregulation of well-known target genes such as GLUL or LGR5 [42]. Compared with proliferative HCC, this type of HCC has a relatively low level of a-fetoprotein and a relatively low degree of malignancy.

The characteristics of proliferative and non-proliferative subtypes are summarized in the Table below, some data mainly sourced from the review reports by Daniela Sia et al. [43] and Jessica Zucman-Rossi et al [35].

Summary of molecular classification of HCC

	Proliferation	Nonproliferation
Cell lineage features	Progenitor-like, Hepatocyte-like	Hepatocyte-like
Activation of signaling pathways	NOTCH mTOR RAS/MAPK	Classical Wnt (CTNNB1 mutation)
Clinical Features	HBV High AFP Poor prognosis	HCV, Alcohol Low AFP Better prognosis
Others	More vascular invasions	Immune related gene signature

1.2 Antibiotics and Tigecycline

Chemotherapy is a highly essential treatment for cancers in advanced stages and its history can be traced back to the twentieth century [44]. However, it caused life-threatening side effects and led to the development of resistance in cancer cells. Currently, there are many categories of chemotherapy agents, including anti-microtubule drugs, inhibitors of mitotic and topoisomerase, alkylating drugs, cytotoxic antibiotics, antimetabolites and corticosteroids. One rather new category are antibiotics.

1.2.1 Antitumor effects of antibiotics

For many years, antibiotics have been used to target bacterial infections. However, during years of clinical practice, antibiotics have been found to have an inhibitory effect on tumors. In recent years more and more basic studies have demonstrated the antitumor effect of antibiotics.

Some antibiotics are powerful intercalating agents, whereas others are DNA-damaging agents. DNA is one of the major molecular targets of many chemotherapeutic agents and is largely considered a non-specific target of cytotoxic agents [45]. Anthracyclins, bleomycins, mitomycins are a few anticancer antibiotics used in therapy. Doxorubicin and daunorubicin are two of the first anthracyclines discovered, which were obtained from Streptomyces and are now widely used in breast cancer as an intercalating agent that can interfere with DNA interactions [46]. Bleomycin prevents DNA repair and causes DNA damage [47]. Mitomycin, a broad-spectrum antibiotic, acts as a bioreductive alkylating agent, which forms covalent linkages with DNA and interferes with DNA synthesis [48].

Next, I will introduce several new antibiotics used in antineoplastic therapy. We believe that further exploration of the anti-tumor effects of antibiotics could provide more new options for the treatment of oncological diseases.

Salinomycin

Salinomycin (SAL), molecular structure is shown in Figure 3, is an antibacterial and coccidiostat ionophore therapeutic drug. SAL is isolated from Streptomyces albus and belonging to the polyether class. It has a wide range of biological activities [49].

SAL has been shown to have proliferation-inhibiting effects in a variety of tumors. The main mechanism including inhibition of Akt, Wnt/β-catenin, hedgehog, and Notch pathways [50, 51]. It has been shown that SAL can

induce apoptosis by altering the balance of NA^+/K^+ ions at the mitochondrial and cellular membranes [52]. Thereafter, SAL have been shown to destroy cancer stem cells in some malignancies and to promote the effects of radiotherapy and chemotherapy [53]. At the same time, SAL has shown striking results in targeting cancer stem cells. It has been reported that SAL has more than 100 times the ability to remove cancer stem cells compared to paclitaxel [54]. In addition to solid tumors, SAL has also been reported to act on hematologic tumors, with the main mechanism being the inhibition of the Wnt pathway [55].

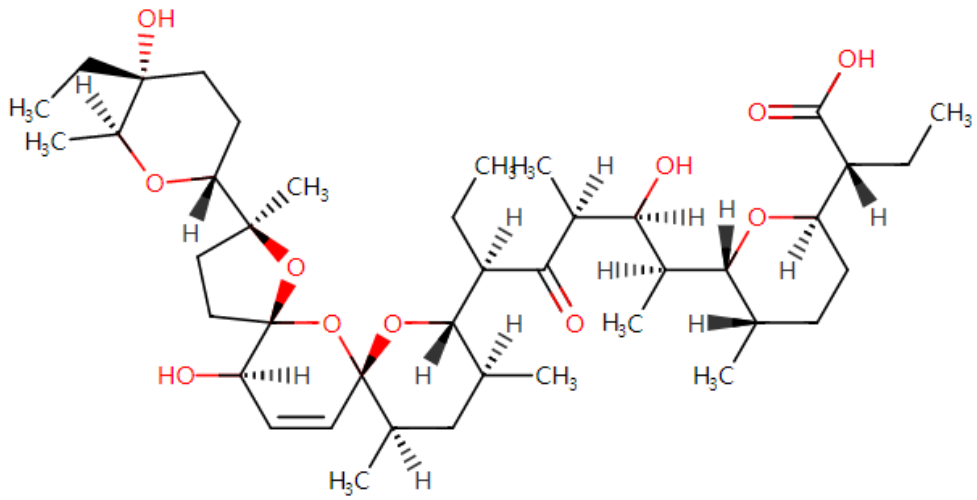

Figure 3: The chemical structure of Salinomycin.

Chemical formula structure figure from the public database Drugbank (https://go.drugbank.com/)[56].

Ivermectin

Ivermectin (IVR) is a semi-synthetic antiparasitic medication derived from avermectins (Figure 4), a class of highly-active broad-spectrum antiparasitic agents isolated from the fermentation products of Streptomyces avermitilis. In the context of the COVID-19 global pandemic, some inhibitory effects of ivermectin on COVID-19 have been reported [57].

IVR exhibited antitumor effects mainly in colon cancer, glioma, skin and lung cancers through the Wnt pathway blocking [58]. In addition to the inhibition of Wnt-TCF pathway, the inhibition of multidrug resistance (MDR) proteins, the blockage of AKT/mTOR pathway, and the degradation of PAK-1 (p21-activated kinase) are the main pathways [59, 60]. In gastric cancer IVR exhibited antitumor effects through the inhibition of YAP-1 [61].

Like SAL mentioned previously, IVR inhibits cancer stem cells in breast cancer [58] and increases the production of intracellular ROS, resulting in some inhibition of breast cancer. Also, in breast cancer Dou et al. found that IVR could induce autophagy in breast cancer [62].

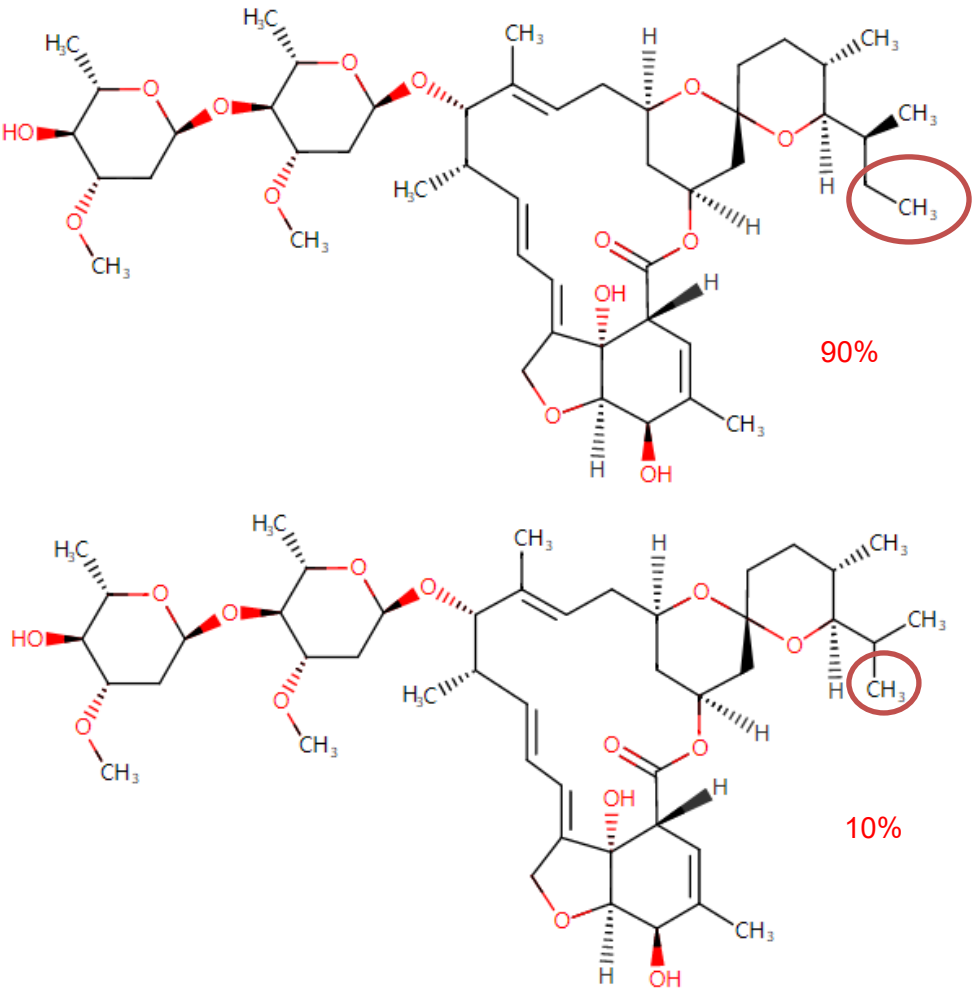

Figure 4: The structure formula of Ivermectin.

Ivermectin itself is a mixture of two avermectins. The two component chemicals are extremely similar, ivermectin B1a has an ethyl group at the C-26 position, while ivermectin B1b has a methyl group. IVR is composed of at least 90% of B1a and not more than 10% of B1b. The red circles show the different structure of the two. Chemical formula structure figure from the public database Drugbank (https://go.drugbank.com/)[56].

Monensin

Monensin (MON), molecular structure is shown in Figure 3, is a polyether isolated from Streptomyces cinnamonensis that presents antibiotic properties [49]. Proven antibacterial and antiparasitic abilities [63]. It is widely used in ruminant animal feeds [64].

MON has been reported to induce apoptosis in a variety of tumors, including renal cell carcinoma [65], colon cancer [66], myeloma [67], and acute myelogenous leukemia [68]. Moreover, the induction of apoptosis in these tumors is associated with cell cycle arrest. MON suppresses signaling pathways associated to cancer formation, including as NF-κB and STAT, and also decreases EGFR expression [69]. Therefore, MON has also been reported to have synergistic effects with many known chemotherapeutic agents (oxaliplatin [69], gemcitabine and erlotinib [70]). MON was selected from 4910 drug-like molecular screens by high-throughput technology and inhibited prostate cancer proliferation even at nanomolar concentrations [71]. Similarly, MON (only at a concentration of 10 nM) induced apoptosis, cell cycle arrest and increased reactive oxygen species (ROS) in prostate cancer cells TEM4-18. Again, this report points out that MON is a selective cytotoxic compound for Epithelial-to-mesenchymal transition [72].

In conclusion MON deserves more further study as a new anti-cancer drug candidate.

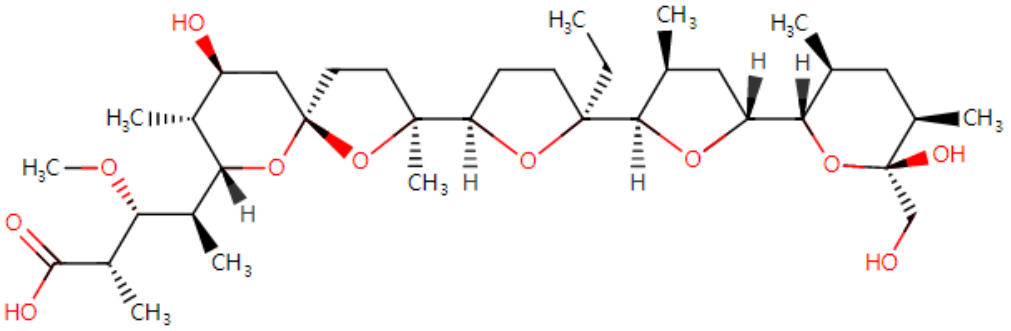

Figure 5: The chemical structure of Monensin.

Chemical formula structure figure from the public database Drugbank (https://go.drugbank.com/)[56].

Above, I have briefly introduced the anti-cancer effects of three antibiotics. Although none of them are currently approved for use in clinical practice, they still deserve to be investigated in greater depth. Over the last decade, there has been a greater awareness of the repositioning of well-known medications, such as antibiotics, as antineoplastic agents. More clinical trial data on the effectiveness of antibiotics repurposed as anticancer medicines are forthcoming. More clinical study data on their effectiveness are expected.

Tigecycline, which we studied next, like the three previous mentioned antibiotics, has been clearly shown to have antitumor effects. However, the specific mechanism, especially in hepatocellular carcinoma, has not been clearly studied. The aim of our project is to fill this part of the gap.

1.2.2 Exploring the antitumor effects and mechanisms of Tigecycline

Tigecycline, a glycylcycline antibiotic drug, plays a huge role in the process of fighting bacterial infections. Its main target is the 30S subunit of the ribosome. It was originally developed to cope with the rising rates of antibiotic

resistance in Staphylococcus aureus, Escherichia coli and Acinetobacter baumannii [73] and got fast-track approval from the FDA on June 17, 2005 [74]. As a broad-spectrum antibiotic, Tigecycline inhibits protein synthesis. It exhibits an antimicrobial effect by binding to the 30S ribosomal subunit of bacteria, which interrupts the interaction of aminoacyl-tRNA with the ribosomal A site [75].

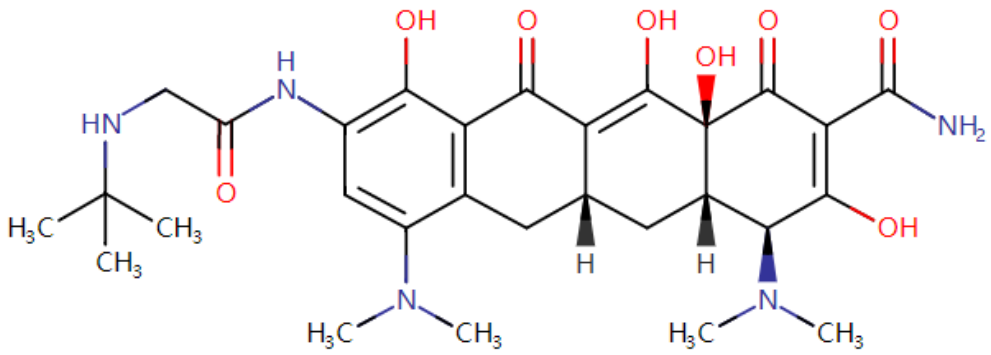

Figure 6: The chemical structure of Tigecycline

Chemical formula structure figure from the public database Drugbank (https://go.drugbank.com/)[56].

Tigecycline has been firstly shown to have anticancer effects in studies of human acute myeloid leukemia, primarily by inhibiting mitochondrial translation [76]. Since then, there have been an increasing number of anticancer studies on Tigecycline. Tigecycline has shown some anti-cancer effect in various solid tumors, including stomach cancer [77], mammary tumors [78], cervical cancer [79], liver cancer [80], lung cancer [81], oral squamous cell carcinoma [82], and Glioma [83], among others.

There are various studies on the mechanism of Tigecycline tumor suppression. We found that these studies are mainly focusing on mitochondrial function in explaining the antitumor mechanism of Tigecycline. Most of these

articles suggest that Tigecycline attenuates mitochondrial function or interferes with mitochondrial translation. In terms of reports on mitochondrial function, major studies have indicated that Tigecycline inhibits mitochondrial oxidative phosphorylation [81, 84, 85], affects mitochondrial biogenesis [76] or induces mitochondrial Oxidative damage [86].

In addition to this, cancer cell death caused by Tigecycline could also be explained by the activation of cell death mechanisms such as apoptosis. The most common form of cell death is apoptosis and extracellular stress is the main reason for activating apoptosis. Therefore, the induction of apoptosis is a viable approach for the treatment of tumors [87]. Interestingly, whether Tigecycline induces apoptosis in tumors seems to be dependent on the primary place of the tumor. Previous studies have shown that no significant apoptosis was found in gastric cancer [77], melaoma [88] and glioma [83] treated with Tigecycline at 10 μM. However, some tumor cells treated at specific concentrations showed a significant level of apoptosis due to the release of cytochrome c and activated BCL-2. For example, 50 μM in chronic myeloid leukemia cells [89], 10 μM in NSCLC cells [81] and 1 μM in cervical cancer cells [79]. We believe that such concentration differences and phenotype differences are still mainly due to the heterogeneity of different organs and tissues.

Autophagy is one of the key degradation processes that can function as programmed cell death in cancers [90, 91]. Autophagy can clear misfolded or damaged organelles. Japanese cell researcher Yoshinori Ohsumi has been awarded the 2016 Nobel Prize in Physiology for autophagy. However, the specific pathways of autophagy activation by Tigecycline differ in the available reports. In chronic myeloid leukemia, down-regulation of the PI3K-AKT-mTOR pathway is the main mechanism for Tigecycline to induce autophagy [89]. In both multiple myeloma and gastric cancer, mTOR was found to be activated by increased phosphorylation levels after Tigecycline

treatment, thereby activating the AMPK pathway to induce cellular autophagy [77, 92].

In addition to these more common mechanisms, there are a number of others that have been reported. Other studies suggest that Tigecycline inhibits the AKT pathway [93]. In a number of cancers, Tigecycline causes cell cycle arrest in the G0/G1-phase [77, 88, 94] and inhibits migration/invasion and angiogenesis [95].

Whether Tigecycline has a therapeutic effect on HCC and whether it inhibits HCC growth in vitro remained unclear to date. Also, whether Tigecycline is harmful to normal hepatocytes is a question that needs to be considered. To address this issue and to explore a potential innovative adjuvant therapy option after HCC resection, our study will explore the effect of Tigecycline on the development of HCC cells and initially explores the mechanisms involved.

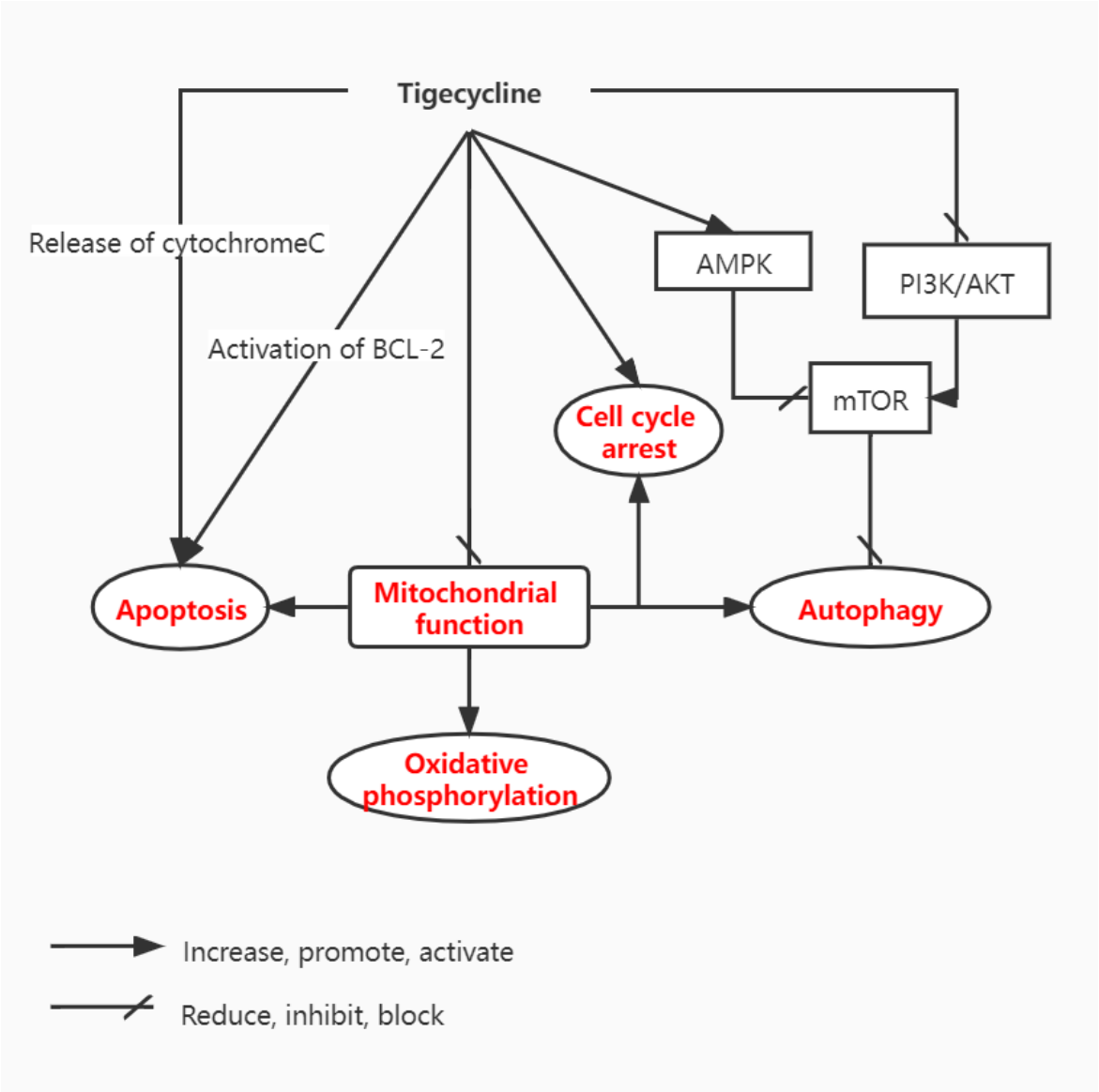

Figure 7. The biological effects of tigecycline in cancer cells.

1.3 Aim of the study

The main aim of the study is to investigate a potential therapeutic role of Tigecycline in HCC in vitro. For this purpose, HCC cells and normal hepatocytes will be treated with Tigecycline and analyses of cytotoxicity, proliferation, cell cycle and apoptosis, as well as of mitochondrial function will be carried out.

2. Materials and Methods

2.1 Materials

2.1.1 Consumables

Consumables	Company or source
6-well plates	Thermo Fisher Scientific, Roskilde,Denmark
12-well plates	Thermo Fisher Scientific, Roskilde,Denmark
96-well plates	Thermo Fisher Scientific, Roskilde,Denmark
5ml pipette	Costar, Maine, USA
10ml pipette	Costar, Maine, USA
25ml pipette	Costar, Maine, USA
50ml pipette	Costar, Maine, USA
1.5ml tips	Eppendorf, Hamburg, Germany
2.0ml tips	Eppendorf, Hamburg, Germany
15ml tube	Falcon, Reynosa, Mexico
50ml tube	Falcon, Reynosa, Mexico
Blot paper	Bio-Rad, California, USA
Cell culture flask T25	Thermo Fisher Scientific, Roskilde,Denmark
Cell culture flask T75	Thermo Fisher Scientific, Roskilde,Denmark

Cell culture flask T125	Thermo Fisher Scientific, Roskilde,Denmark
Cell scraper	TPP, Trasadingen, Switzerland
FACS tubes	Falcon, New York, USA
Filter paper	Whatman, Maidstone, UK
Polyvinylidene difluoride membranes	Merck Group, Darmstadt, Germany
Low-attachment 96-well plates	Corning, Krailling, Germany
Seahorse kit	Agilment, California, USA
Transwell plates	Corning, New York, USA

2.1.2 Chemicals

Chemicals	Company or source	Identifier
β -Mercaptoethanol	Sigma-Aldrich, Steinheim, Germany	M6250
Agarose	Life science, leuven, Belgium	18J034129
Ammonium persulfate (APS)	Serva, Heidelberg, Germany	13376.01
BSA	Biomol, Plymouth Meeting, USA	9048-46-8
B27	Gibco, New York, USA	Cat#12587-010
BEGM	Lonza, Basel, Switzerland	Cat#: CC-3170
Crystal violet	Sigma-Aldrich, Steinheim, Germany	C0775

6X DNA Sample Loading Buffer	Thermo Fisher Scientific, Schwerte, Germany	R0611
30% PolyAcrylamid	Carl Roth, Karlsruhe, Ger-many	Art.-Nr 3029.1
DCFH-DA	Sigma-Aldrich, St. Louis, Missouri, USA	4091-99-0
DMSO	Sigma-Aldrich, Karlsruhe, Germany	D2650
DMEM/F12	Gibco, New York, USA	11330-032
DNA–Ladder standard	Invitrogen, California, USA	10787-018
Everolimus	Selleckchem, Munich, Germany	Cat#S1120
EGF	ImmunoTools, Friesoythe, Germany	Cat#11343406
ECL™ Western Blotting Detection System	Bio-Rad Laboratories, California, USA	102031594 102031597
80% Ethanol	Apotheke GH, Munich, Germany	603-002-00-5
>99% Ethanol	PanReac AppliChem, Germany	0v013438
FBS	Sigma-Aldrich, Steinheim, Germany	35079017
FGF	ImmunoTools, Friesoythe, Germany	Cat#11343623

200mM Glutamine	PAN-Biotech, Baryern, Germany	Cat#P04-80100
1M Glucose	Agilment, California, USA	Cat#103577-100
Hydrogen peroxide 30%	Merck, Darmstadt, Germany	K42389487 135
Loading buffer 4x	Bio-Rad, California, USA	161-0747
Methanol	Merck, Darmstadt, Germany	1.06009.1000
MTT powder	Thermo Fisher Scientific, Massachusetts, USA	2216966
Matrigel	Sigma-Aldrich, Steinheim, Germany	06693
Methyl cellulose	Sigma-Aldrich, Steinheim, Germany	Lot BCCB8250
Opti-MEM™	Thermo Fisher Scientific, Massachusetts, USA	31985070
PBS	PAN-Biotech, Munich, Germany	P04-36500
100mM Pyruvate	Agilment, California, USA	Cat#103578-100
Protein standards	Bio-Rad, California, USA	RB227155
Protease inhibitor cocktail	Roche, Basel, Switzerland	05892791001
Phospho Stop cocktail	Roche, Basel, Switzerland	04906837001

10X Tris/Glycine/ SDS buffer (Running buffer)	Bio‐Rad Laboratories, Cali-fornia, USA	Cat#1610772
RNase-free water	Qiagen, Hilden, Ger-many	129112
RPMI 1640 Medium	Gibco, New York, USA	21875-034
RIPA lysis buffer 10X	Millipore, Darmstadt, Germany	20-188
Seahorse XF Medium	Agilment, California, USA	14620003
SDS	Carl Roth, Karlsruhe, Germany	2326.2
Tigecycline	Apotex Inc., Toronto, Ontario, Canada	NDC 60505-6098-0
TEMED	Thermo Fisher Scien-tific, Massachusetts, USA	17919
Transfer Buffer (20X)	Novex, Van Allen Way Carlsbad, CA	BT00061
Tris Base	Carl Roth, Karlsruhe, Ger-many	9090.3
Trypan blue	Sigma-Aldrich, Stein-heim, Germany	T8154
Trypsin/EDTA	Lonza, St. Louis, USA	BE17-161E
Tween 20	Sigma-Aldrich, Heidel-berg, Germany	P1379

2.1.3 Antibodies

Primers	Company or source	Identifier
RAC1	Cell Signaling Technology, Massachusetts, USA	cat. no. 4561
ERK1/2	Cell Signaling Technology, Massachusetts, USA	# 9102S
P-ERK1/2	Cell Signaling Technology, Massachusetts, USA	# 9101S
OXPHOS	Abcam, Massachusetts, USA	ab110411
GAPDH	Santa Cruz Biotechnology, Texas, USA	Cat#sc-25778

2.1.4 Primers

Primers	Company or source	Identifier
RAC1	Qiagen, Hilden, Germany	Cat#QT00065856
GAPDH	Qiagen, Hilden, Germany	Cat#QT00079247

2.1.5 Commercial Assays kits

Product	Company or source	Identifier
BCA protein Assay kit	Thermo Fisher Scientific, Schwerte, Germany	Cat# 23227

BEGM BulletKit™	Lonza, Basel, Switzerland	Cat#: CC-3170
BrdU cell cycle kit	BD Pharmingen, San Diego, CA	Cat# 559619
FlexiTube siRNA -Rac1	Qiagen, Hilden, Germany	Cat# 1027417
Lipofectamine RNAiMAX	Invitrogen, California, USA	Cat#13778-100
QuantiNova ™ SYBR Green PCR Kit	Qiagen, Hilden, Germany	Cat#208154
Reverse-transcribed kit	Thermo Fisher Scientific, Schwerte, Germany	Cat#11756050
RNA isolate kit	Qiagen, Hilden, Germany	Cat#74904
Seahorse assay kit	Agilment, California, USA	103591-100

2.1.6 Apparatus

Apparatus	**Company or source**
Autoclave	Unisteri, Oberschleißheim, Germany
Bio-Rad CFX96 Real-Time PCR system	Bio-Rad Laboratories, California, USA
Centrifuge	Hettich, Ebersberg, Germany
Cool Centrifuge	Eppendorf, Hamburg, Germany
Micro centrifuge	Labtech, Ebersberg, Germany
CO_2 Incubator	Binder, Tuttlingen, Germany

DNA workstation	Uni Equip, Martinsried, Germany
Drying cabinet	Thermo Fisher Scientific, Schwerte, Germany
Electronic pH meter	Knick Elektronische Messgeräte, Berlin, Germany
FACS Fortessa	BD Biosciences, Heidelberg, Germany
Fridge (4℃, -20℃ and -80℃)	Siemens, Munich, Germany
Ice machine	KBS, Mainz, Germany
Inverted light microscope	Nikon, Tokio, Japan
Liquid Nitrogen tank	MVE Goch, Germany
Lamina flow	Thermo Fisher Scientific, Schwerte, Germany
Microscope	Olympus, Hamburg, Germany
Micro weigh	Micro Precision Calibration, California, USA
Pipette boy	Eppendorf, Hamburg, Germany
Trans-Blot Turbo	Bio-Rad Laboratories, California, USA
Thermocycler	Eppendorf, Hamburg, Germany
Thermomixer comfort	Eppendorf, Hamburg, Germany
ChemiDoc Imaging System	Bio-Rad Laboratories, California, USA
Shaker	Edmund Bühler, Bodelshausen, Germany
Seahorse XFp Analyzer	Agilment, California, USA

VersaMax ELISA Microplate Reader	Molecular Devices, California, USA
Vortex Mixer VF2 (Janke & Kunkel)	IKA, North Carolina, USA
Water bath	Memmert, Schwabach, Germany

2.1.7 Software

Software and version	Company
FlowJo Vesion 10.0	BD Biosciences
Graphpad Prism 7.04	GraphPad
ImageJ Version 1.50i	National Institutes of Health

2.1.8 Buffer and Solutions

MTT solution

MTT powder	25mg
PBS	50ml

Western blot

Separating Gel (10% and 13%)

	10%	13%
H_2O	4.1ml	3.1ml
1.5M Tris pH8.8	2.5ml	2.5ml
30% PolyAcrylamid	3.3ml	4.3ml
10% SDS	0.1ml	0.1ml
10% APS	50ul	50ul
TEMED	5ul	5ul

Stacking Gel

H_2O	2.4ml
1.5M Tris pH6.8	1ml
30% PolyAcrylamid	0.6ml
10% SDS	0.04ml
10% APS	20ul
TEMED	4ul

1x Running Buffer

10X Tris/Glycine/ SDS buffer	100ml
H_2O	900ml

1x Transfer Buffer

Transfer Buffer 20x	50ml
Ethanol	150ml
H_2O	800ml

10x TBS

Tris Base	24g
NaCl	80g
H_2O	1000ml
PH	7.6

1x TBS-T

10x TBS	100ml
H_2O	900ml

Tween	1ml

Blocking Buffer

BSA	2.5mg
H_2O	50ml

Protein lysis Buffer

10x RIPA buffer	1ml
H_2O	9ml
Phospho Stop	1 Table
Protease Inhibitor	1 Table

1M Tris-HCl

Tris-base	12.12g
H_2O	200ml
PH	6.8

1.5M Tris-HCl

Tris-base	36.34g
H_2O	200ml
PH	8.8

Loading buffer

4xloading buffer	3600ul
β -Mercaptoethanol	400ul

10%SDS

SDS	10g
H_2O	100ml

10%APS

APS	10g
H_2O	100ml

Crystal violet solution

Crystal violet	500mg
Methanol	20ml
H_2O	80ml

Seahorse assay medium

Seahorse XF Medium	970ul
1M Glucose	100ul
100mM Pyruvate	100ul
200mM Glutamine	100ul

2.2 Methods

2.2.1 Cell culture

2.2.1.1Hepatocellular carcinoma cells (Huh7 and HepG2)

The two HCC cell lines Huh7 and HepG2 were purchased from ATCC and stored in bio-liquid nitrogen tanks in the laboratory of the department of

General, Visceral, and Transplantation Surgery, Ludwig Maximilians-University. The two HCC cell lines utilized and cultured in RPMI 1640 medium, supplemented with 10% fetal bovine serum (FBS), in a humidified incubator with 5% CO_2 at 37 ℃. Change the culture medium every 3 days.

2.2.1.2Liver normal immortalized cells (THLE-2)

THLE-2 human normal liver epithelial cells were purchased from the American Type Culture Collection (ATCC) and cultured in BEGM (Bronchial Epithelial Cell Growth Medium). The BEGM kit includes 500 mL basal medium and separate frozen additives from which we discard the gentamycin/amphotericin (GA) and epinephrine and to which we add extra 5 ng/ml EGF, 70 ng/ml phosphoethanolamine and 10% FBS. The cell culture flasks used were precoated with a mixture of 0.01 mg/ml fibronectin, 0.03 mg/ml bovine collagen type I and 0.01 mg/ml bovine serum albumin dissolved in BEBM medium.

All cells were routinely tested for mycoplasma according lab rules every four months authenticated commercially by IDEX BioResearch once a year (Ludwigsburg, Germany).

2.2.2 Cell viability assay

2.2.2.1MTT

Cell viability was assessed using a 3-(4,5-Dimethylthiazol-2-yl)-2,5-Diphenyltetrazolium Bromide assay (Thermo Fisher Scientific, Waltham, Massachusetts, USA). According to the manufacturer's instructions, cells were plated at a density of $8x10^4$/well in 96-well plates with different concentrations of Tigecycline and cell viability was assessed at different timepoints. The absorbance of each well was measured at a wavelength of 570 nm with a background wavelength of 670 nm using VersaMax microplate reader

(Molecular devices Instruments, San Jose, California, USA). Empty wells served as blank controls. The test was performed three times under the same operating conditions. The standard curves were obtained according to Non-linear Regression in GraphPad Prism 7.04 software, and then the half maximum inhibitory concentrations (IC_{50}) of Tigecycline on different cells were calculated.

2.2.2.2 Crystal violet staining

To verify the experimental results, we continued to test cell viability of the same batch of samples with crystal violet (CV). Cells were seeded and treated as in the MTT experiment and $8x10^4$ cells were seeded in 96-well plates. The cells were washed with PBS to ensure that all medium was removed. 50 µl of 4% paraformaldehyde (PFA) were added and an incubation for 15 minutes at room temperature followed. PFA was discarded and it was allowed to air dry for 15 to 20 minutes. Then, cells were stained with 50 µl of CV solution for 15 minutes. After discarding the CV, the cells were washed with H_2O and it was allowed to dry overnight at room temperature. The next day, the dye was dissolved in 50 µl of 33% acetic acid. The absorbance of the developed color was measured at a wavelength of 570 nm with a background wavelength of 670 nm using VersaMax microplate reader. The cell viability was calculated as a comparative percentage to the values obtained from untreated cells.

2.2.3 Detection of ROS

The intracellular level of reactive oxygen species (ROS) in form of cellular peroxides was assessed using a 10 µmol/l 2',7'-dichlorofluorescein diacetate (DCFH-DA, Sigma-Aldrich, St. Louis, Missouri, USA) as a probe after treatment with Tigecycline or hydrogenperoxide. In the Tigecycline treatment group, the cells were treated with different concentrations of Tigecycline for 24 hours. Cells were collected and suspended in diluted DCFH-DA at a cell

concentration of 20,000 cells/ml and incubated for 30 minutes at 37 °C. The suspension was mixed upside down every 3 to 5 minutes to bring the probe and cells into full contact. Cells were washed three times with serum-free cell culture medium to adequately remove DCFH-DA that has not entered the cells. In the positive control group, cells were treated with 70% hydrogenperoxide for 1 hour after loading the probes. Cells were collected and assayed with a Filter Max F3 microplate reader (Molecular devices Instruments, San Jose, California, USA). The detection parameters were 488 nm excitation wavelength and 525 nm emission wavelength.

2.2.4 Western blot analysis

Huh7, HepG2 and THLE-2 cells were washed twice with cold PBS and harvested with protein lysis buffer including protease and phosphatase inhibitors (Roche, Basel, Switzerland). The protein concentrations were assessed using a BCA Protein Assay kit (Thermo Fisher Scientific, Schwerte, Germany). Equal amounts of proteins (25 µg/lane) from each group were separated by sodium dodecyl sulfate polyacrylamide gel electrophoresis on 10% and 13% gels (Bio-Rad Laboratories, Hercules, California, USA) and transferred to polyvinylidene difluoride membranes (Merck Group, Darmstadt, Germany). After blocking with 5% bovine serum albumin (BSA) for 1 hour at room temperature, the membranes were incubated with specific primary antibodies at 4°C overnight. Then, after washing three times with tris-buffered saline containing Tween-20 (TBST), the membranes were incubated with horseradish peroxidase-conjugated secondary antibodies for 1 hour at room temperature. Proteins were visualized by chemiluminescence using enhanced chemiluminescent substrate (Bio-Rad Laboratories, Hercules, California, USA). Immunoreactive bands were examined using the ChemiDoc Imaging System (Bio-Rad Laboratories, Hercules, California, USA). The

following antibodies were used: Rabbit Rac1/Cdc42 antibody (Cell Signaling Technology, Danvers, Massachusetts, USA; cat. no. 4561, dilution 1:1000). Rabbit p44/42 MAPK (Erk1/2) (Cell Signaling Technology, Danvers, Massachusetts, USA; cat. no. 4695, dilution 1:1000). Rabbit Phospho-p44/42 MAPK (Erk1/2) (Cell Signaling Technology, Danvers, Massachusetts, USA; cat. no. 8544, dilution 1:1000). GAPDH antibody (Santa Cruz Biotechnology, Texas, USA, Cat#sc-25778). Mouse OXPHOS antibody, (Abcam, ab110411). GAPDH was used as an internal control for each membrane.

2.2.5 Sphere formation assay

The human cell lines Huh7 and HepG2 were cultured in suspension in sphere formation assay (SFA) medium which consisted of serum-free DMEM/F12 supplemented with B27 (Gibco, New York, USA; 1:50), 10 ng/ml epidermal growth factor (EGF) and 20 ng/ml basic fibroblast growth factor (bFGF) (ImmunoTools, Friesoythe, Germany) and 1% methylcellulose. To form hepatocellular carcinoma spheres, 1000 suspended cells were cultured per well in ultra-low attachment plates (Corning, Corning, New York, USA). After 8 days of treatment the formed spheres were inspected under the microscope and pictures were taken with 40x magnification. The amount of clones and clones' size were then analyzed by ImageJ software (open source software).

2.2.6 Wound healing assay

Huh7 and HepG2 cells were seeded in 6-well plates. When the cells grew in a full monolayer, a wound was produced by scraping straight across the cell monolayer using a 200 µl sterile tip. The cells were then washed gently with PBS and new serum-free medium was added. Pictures were taken immediately (0 h). Further pictures were taken again in the same location and with

the same magnification after 24 and 48 hours. The area of each wound was analyzed at different time points using ImageJ software (open source software). The reduction of the wound area was then calculated and interpreted as cell migration ratio.

2.2.7 Transwell assay

Matrigel and serum-free medium were dissolved at 4 °C in a 1:3 ratio, mixed thoroughly and added to the upper chamber of the transwell plate. 40 µl were added to each chamber so that it fully covered the bottom of the chamber. Then it was put into the incubator with 5% CO_2 at 37 °C overnight to allow the Matrigel to solidify fully. A total number of 100,000 cells in 300 µl serum-free medium were seeded into the upper chamber of the 8.0 µm pore size transwell plate (Corning, New York, USA) and 600 µl complete medium was added to the lower compartment. The cells were incubated for 24 hours in a humidified incubator with 5% CO_2 at 37 °C. After incubation for 24 hours the upper chamber was wiped twice with cotton swabs. Next, cells were fixed with 4% paraformaldehyde for 15 to 20 minutes and stained with 0.5% CV for another 15 to 20 minutes at room temperature. The numbers of invading cells in 3 randomly selected fields were counted under an inverted light microscope (TE2000-U Inverted Microscope, Nikon, Tokio, Japan; 100x magnification). Three replicates were performed the number of invading cells under different conditions demonstrate the effect on the invasion ability of the used cells.

2.2.8 Mitochondrial bioenergetics measurements

To assess mitochondrial respiratory function, mitochondrial oxygen consumption rates (OCR) were analyzed using the Seahorse XFp Analyzer. Huh7, HepG2 and THLE-2 were seeded in Seahorse 8-well mini-plates

(12,000 cells/well) and cultured at 37 ℃ with 5% CO_2 and treated with different concentration of Tigecycline for 48 hours. After 48 hours treatment day, media was replaced with Seahorse assay medium, cells were incubated at 37 ℃ without CO_2 for 1 hour and then 2 μM oligomycin and 0.5 μM rotenone/antimycin A were added sequentially to assess mitochondrial respiratory capacity. For short-term treatment of Huh7, HepG2 and THLE-2, cells were treated and measured them on the same day. Cells were cultured in medium with Tigecycline in Seahorse 8-well mini-plates for 6 hours. After 6h treatment, the medium with Tigecycline replaced with seahorse analysis medium and then performing subsequent experiments. Also, mitochondrial basal respiration, ATP-production and proton leak could be performed as manufacture's protocol.

2.2.9 Flow Cytometric Analysis of Cells

Flow cytometry and BrdU Flow kits (BD Pharmingen, San Diego, CA) was used to analyze the cell cycle changes of three cells after Tigecycline treatment. Firstly, labeling cells in vitro. Carefully add 20 μl BrdU solution (1 mM BrdU in 1xDPBS) directly to 2ml of culture medium and incubate 1h. Then, trypsinase cells from well and put it in a FACS tube, centrifuge for 5 minutes at 200 to 300 g, discard supernatant. Resuspend in 100μl BD Cytofix/Cytoperm Buffer, incubate for 30 minutes at room temperature. After washing with 1ml 1xBD Perm/Wash buffer, resuspending cells in 100 μl BD Cytoperm Permeabilization Buffer Plus, incubating for 10 minutes on ice. Measurements were performed by flow cytometry immediately after staining the cells with fluorescent anti-BrdU and 7-AAD solution, respectively, according to the operator's instructions of the kit.

2.2.10 RNA isolation and real‑time PCR (RT‑PCR)

Total RNA from Huh7 and HepG2 cells was extracted with a total RNA extraction kit (Qiagen, Inc.) and reverse-transcribed using the SuperScript ™ IV VILO™ Master Mix kit (Thermo Fisher, Inc.), Quantitative RT-PCR was performed using QuantiNova ™ SYBR Green PCR Kit (Qiagen, Inc.) in a 20µl PCR mixture on a Bio-Rad CFX96 Real-Time PCR system (Bio-Rad Laboratories, Inc.) according to the manufacturer's standard protocols. RNA samples were reverse-transcribed in a thermocycler with the following protocol: Priming, 25 ℃ for 10 minutes, reverse transcription, 50 ℃ for 10 minutes, inactivation, 85 ℃ for 5 minutes and hold at 4 ℃. The reverse-transcribed reaction settings are shown in Table 1 below. QuantiNova™ SYBR Green PCR Kit was used for RT-RCR assays. The reaction setup of the kit is shown in Table 2 below. The RT-PCR amplification processes were as follows: An initial cycling for 2 minutes at 95℃, followed by 40 cycles at 95 ℃ for 5 seconds and 10 seconds at 60 ℃. Each sample was performed in triplicate and a negative control with sterile RNase free H_2O was used instead of template DNA. Housekeeping gene GAPDH was used to normalize the variation of cDNA. Three independent experiments were performed for each group. Relative gene expression was normalized to GAPDH and calculated using the 2-ΔΔCq method.

Table 1: The reverse-transcribed reaction settings

SuperScript™ IV VILO™ Master Mix	4ul
Template RNA (1pg to 2.5ug to total RNA)	varies
RNase-free water	to 20ul

Table 2: Reaction setup of QuantiNova™ SYBR Green PCR Kit

SYBR Green PCR Master Mix	10ul

QN ROX Reference Dye	2ul
Primer	2ul
RNase-free water	4ul
cDNA	2ul
Total reaction volume	20ul

2.2.11 Bioinformatic analysis

The molecular structure of Tigecycline was obtained from PubChem (https://pubchem.ncbi.nlm.nih.gov/). Information on a total of 6,876 HCC-related genes was retrieved from the GeneCards database using “hepatocellular carcinoma” as keyword. According to a GeneCards Inferred Functionality Score (GIFtS) greater than 20, we selected the top 5.4% of genes, which comprised a total of 376 genes. Similarly, a search in the Disgenet database (https://www.disgenet.org/) using “hepatocellular carcinoma” as a keyword comprised 96 potential genes for hepatocellular carcinoma. Excluding the 43 genes contained in both databases, a total of 429 potential genes related to hepatocellular carcinoma were obtained. Genes associated with Tigecycline were obtained from the PharmMapper (http://www.lilab-ecust.cn/pharmmapper/) database and the Comparative Toxicogenomics Database (CTD, http://ctdbase.org/). Hereby 34 genes were got. After analysis, 11 potential targets related to both HCC and Tigecycline were identified. KEGG (Kyoto Encyclopedia of Genes and Genomes) enrichment analysis was performed to determine the pathways significantly associated with the 11 potential target genes. Survival data for 11 potential genes was retrieved from the Kaplan-Meier plotter (https://kmplot.com/analysis/). Data for differential gene expression were obtained from GEPIA (http://gepia.cancer-pku.cn/) and The Human Protein Atlas (https://www.proteinatlas.org/).

2.2.12 Statistical analysis

All experiments were independently performed at least three times. The mean standard deviation (SD) was determined for each group. Statistical analyses were performed using one/two-way analysis of variance (ANOVA) for multiple group comparisons or student's t-test for individual comparisons. Statistical significance was considered at $p<0.05$. In all statistical graphs, bar graphs represent the mean ± SD. *P<0.05, **P<0.01, ***P<0.005, ****P<0.001 and ns means no significance compared with the control group.

3. Results

3.1 Tigecycline shows antitumor effect on HCC cells

To investigate the effects of Tigecycline on HCC, two different human HCC cell lines (HepG2 and Huh7) were used. Both HCC cell lines were treated with different concentrations of Tigecycline for 24 and 48 hours. The viability of HCC cells after Tigecycline treatment for 24 and 48 hours was detected by MTT assays. After 24 hours, the decrease in viability of Huh7 cells was not significant with the increase of Tigecycline treatment concentration. However, after 48 hours, the decrease of viability of Huh7 was very significant with the increase of Tigecycline treatment concentration (Fig. 8 A and C). Similar results were obtained in HepG2 cells (Fig. 8 B and D). To further confirm the results of 48 hours, we tested the viability of both HCC cell lines again with Crystal violet (CV) staining and got the similar results as MTT assays (Fig. 8 E and F). To clarify whether there is a difference in the cytotoxicity of Tigecycline between the two HCC cell lines, we calculated the half maximal inhibitory concentration (IC_{50}) of the two cell lines. The results showed that the IC_{50} of the two cell lines were indeed different. HepG2 with a calculated and MTT based IC_{50} of 1,723 µM was more sensitive than Huh7 with an IC_{50} of 7,695 µM for Tigecycline.

To further examine the effect of Tigecycline, we performed sphere formation assays to create stem cell like HepG2 and Huh7 cells in three-dimensional culture. Size and number of spheres were analyzed using ImageJ software after Tigecycline treatment (Fig. 8 G and J). The software analysis showed a reduction in count and size of spheres in both HCC cell lines (Fig. 8 H, I, K and L). Again, the sensitivity varied for the two different HCC cell lines. Especially regarding clone count, Huh7 was more sensitive to Tigecycline in the three-dimensional culture.

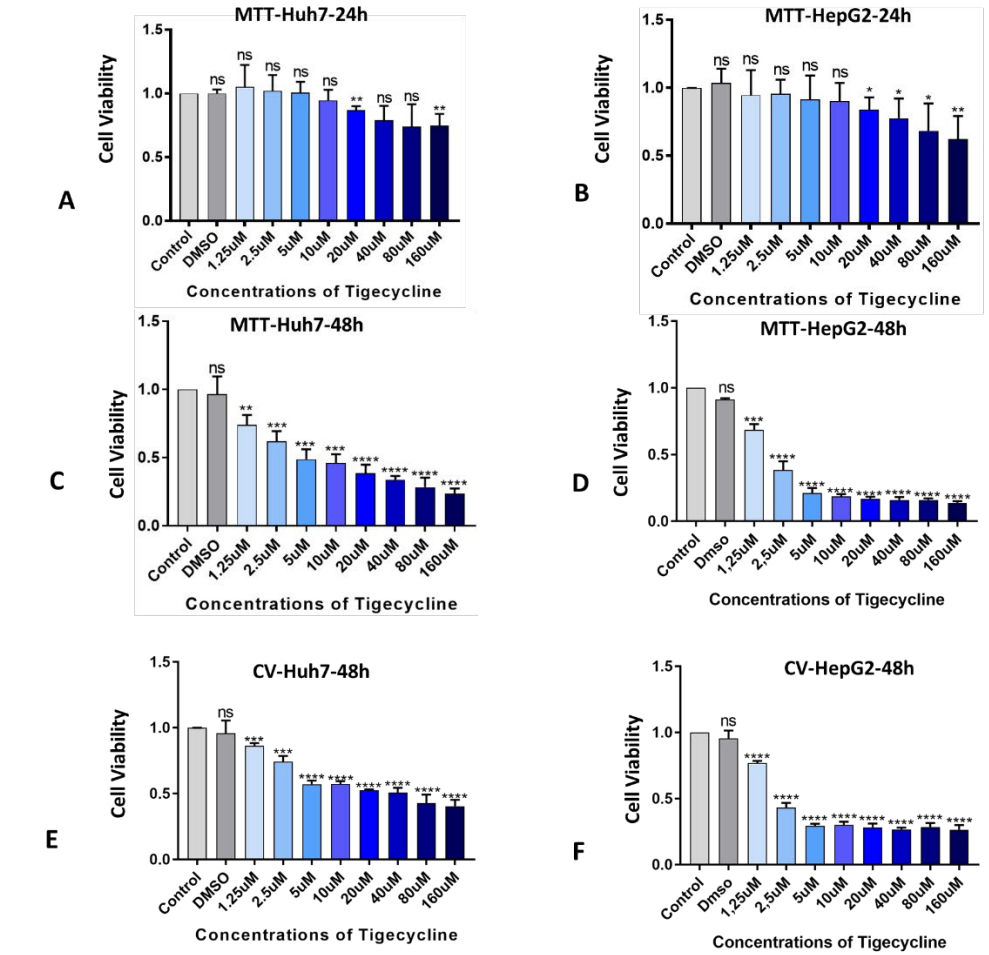
A
MTT-Huh7-24h
Cell Viability
Concentrations of Tigecycline
B
MTT-HepG2-24h
Cell Viability
Concentrations of Tigecycline
C
MTT-Huh7-48h
Cell Viability
Concentrations of Tigecycline
D
MTT-HepG2-48h
Cell Viability
Concentrations of Tigecycline
E
CV-Huh7-48h
Cell Viability
Concentrations of Tigecycline
F
CV-HepG2-48h
Cell Viability
Concentrations of Tigecycline
Control
DMSO
1.25uM
2.5uM
5uM
10uM
20uM
40uM
80uM
160uM

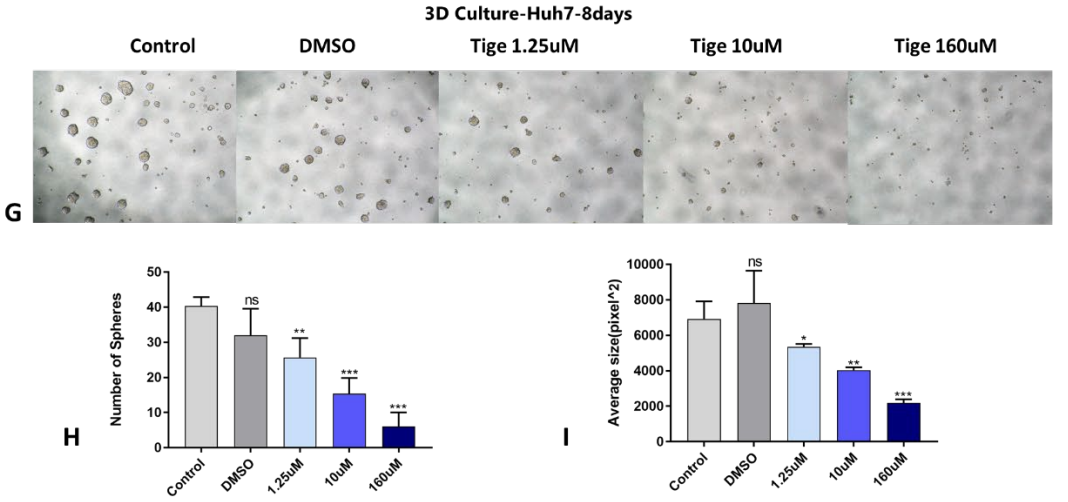
3D Culture-Huh7-8days
Control
DMSO
Tige 1.25uM
Tige 10uM
Tige 160uM
G
H
Number of Spheres
I
Average size(pixel^2)
3D Culture-HepG2-8days
Control
DMSO
Tige 2.5uM
Tige 10uM
Tige 40uM
J
K
Number of Spheres
L
Average size(pixel^2)

Figure 8: Cytotoxicity assay Huh7 and HepG2 after Tigecycline treatment and Sphere formation assay Huh7 and HepG2

The two cell lines Huh7 (A) and HepG2 (B) were treated with different concentrations of Tigecycline for 24 hours and cell viability of both cells was measured by MTT, the results of treatment for 48h are shown in (C) and (D); A Crystal Violet assay was used to validate the inhibitory effects of increasing Tigecycline concentrations for Huh7 (E) and HepG2 (F); Sphere formation assays were used to create stem cell like Huh7 and HepG2 cells in a three-dimensional cell culture model; Images of Huh7 (G) and HepG2 (J) cells after 8 days of incubation with different concentration of Tigecycline under microscope with a magnification of 100x; Statistical analysis of the number of spheres (H, K) and size of spheres (I, L) for sphere formation of Huh7 (H, I) and HepG2 (J, K) after 8 days of incubation with different concentration of Tigecycline was performed using the image analysis software Image J.

MTT, 3-(4,5-Dimethylthiazol-2-yl)-2,5-Diphenyltetrazolium Bromide; CV, Crystal Violet; Tige, Tigecycline; IC_{50}, half maximal inhibitory concentration.

3.2 Tigecycline inhibits migration and invasion of HCC cells

After confirming the influence of Tigecycline on the viability of HCC cells, we further assessed whether there is a Tigecycline associated effect on migration and invasion of HCC cells. Therefore, we performed wound healing assays to detect the migration of HCC cells (Fig. 9 A and F). After treating Huh7 cells with different concentrations of Tigecycline for 24 hours (Fig. 9 C) and 48 hours (Fig. 9 D), the analysis revealed that even 10 µM Tigecycline can inhibit the migratory ability of Huh7 cells. The inhibition of HepG2 migration was only significant with 80 µM of Tigecycline for 24 hours (Fig. 9 H) and 40 µM for 48 hours (Fig. 9 I). Furthermore, transwell assays with matrigel were used to test invasion ability of Huh7 and HepG2 with increasing Tigecycline concentrations (Fig. 9 B and G). As seen in Fig. 9 B and E, already 10 µM of Tigecycline reduced the number of Huh7 cells invading after 24 hours significantly. Performing the same experiments with the

HepG2 cell line, as displayed in Fig. 9 G and J, we observed comparable inhibition of invasion.

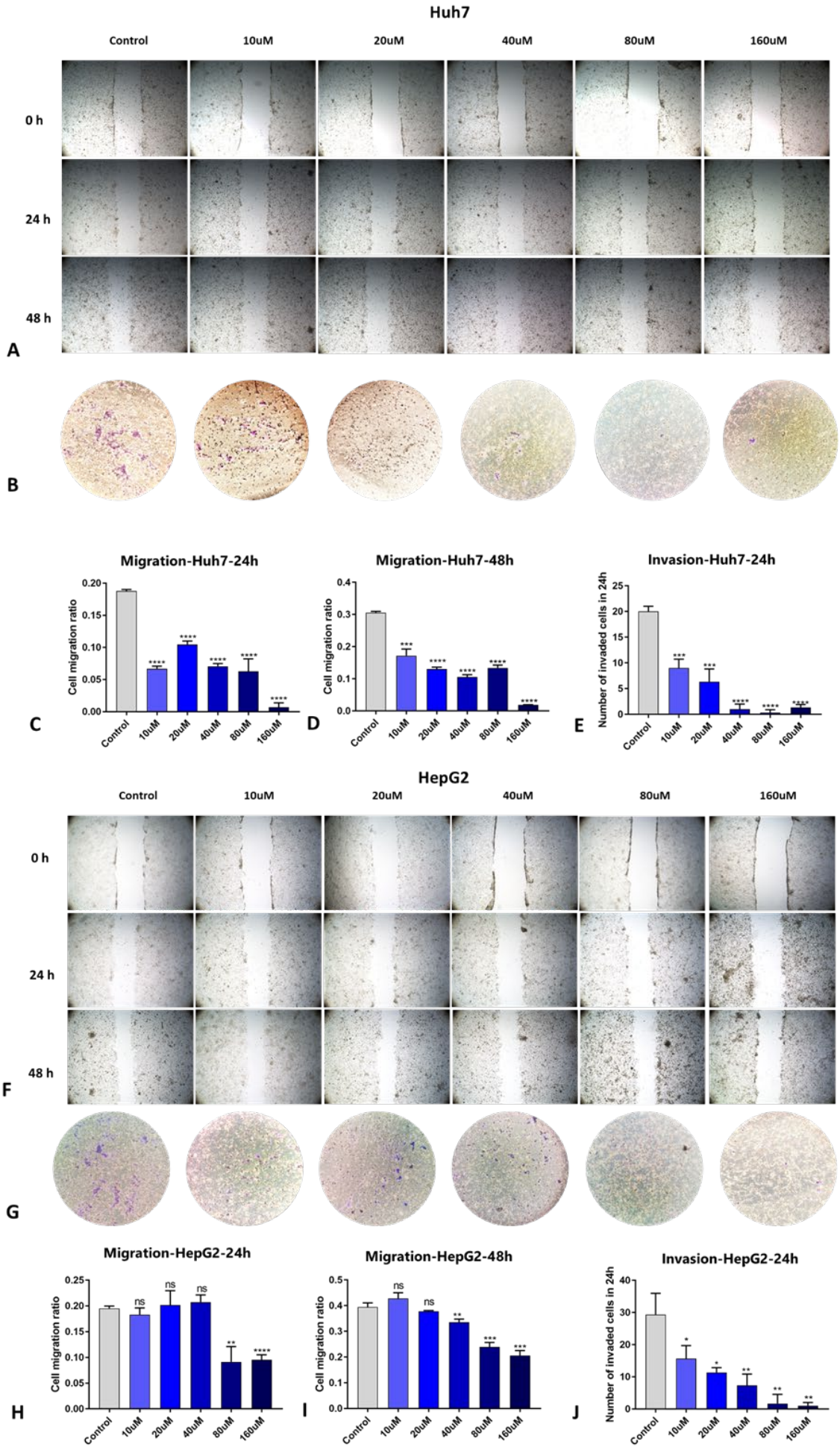
Huh7
Control
10uM
20uM
40uM
80uM
160uM
0 h
24 h
48 h
A
B
Migration-Huh7-24h
Cell migration ratio
C
Migration-Huh7-48h
D
Invasion-Huh7-24h
Number of invaded cells in 24h
E
HepG2
F
G
Migration-HepG2-24h
H
Migration-HepG2-48h
I
Invasion-HepG2-24h
J

Figure 9: Altered migration and invasion of HCC cells with increasing Tigecycline concentrations assessed by wound healing assays and transwell invasion assays with matrigel.

Microscope images at a magnification of 50x at different timepoints of wound healing assays with Huh7 (A) and HepG2 (F) with increasing Tigecycline concentrations; Microscope images at a magnification of 100x of transwell assays with Huh7 (B) and HepG2 (G) with increasing Tigecycline concentrations; Image J based analysis of wound healing images with Huh7 after 24 hours (C) and 48 hours (D); Analysis of transwell invasion images with Huh7 after 24 hours (E); Analysis of wound healing images with HepG2 after 24 hours (H) and 48 hours (I); Analysis of transwell invasion images with HepG2 after 24 hours (J).

3.3 Tigecycline leads to reduced levels of ROS

Previous studies reported that Tigecycline promotes the production of reactive oxygen species (ROS) [80]. Also, the further down mentioned protein RAC1 plays an important role in the intracellular accumulation of ROS [96]. To assess the effect of Tigecycline on ROS in HCC, we used a DCFH-DA assay as described in methods to examine the changes of ROS after treatment with different concentrations of Tigecycline in the cell lines HepG2 and Huh7. The results showed that ROS decreased with increasing Tigecycline concentration after 24 hours of Tigecycline treatment in the two HCC cell lines (Fig. 10 A and C). After 48 hours of treatment, ROS also decreased with increasing Tigecycline concentrations (Fig. 10 B and, D), but increased compared to the same concentration at 24 hours.

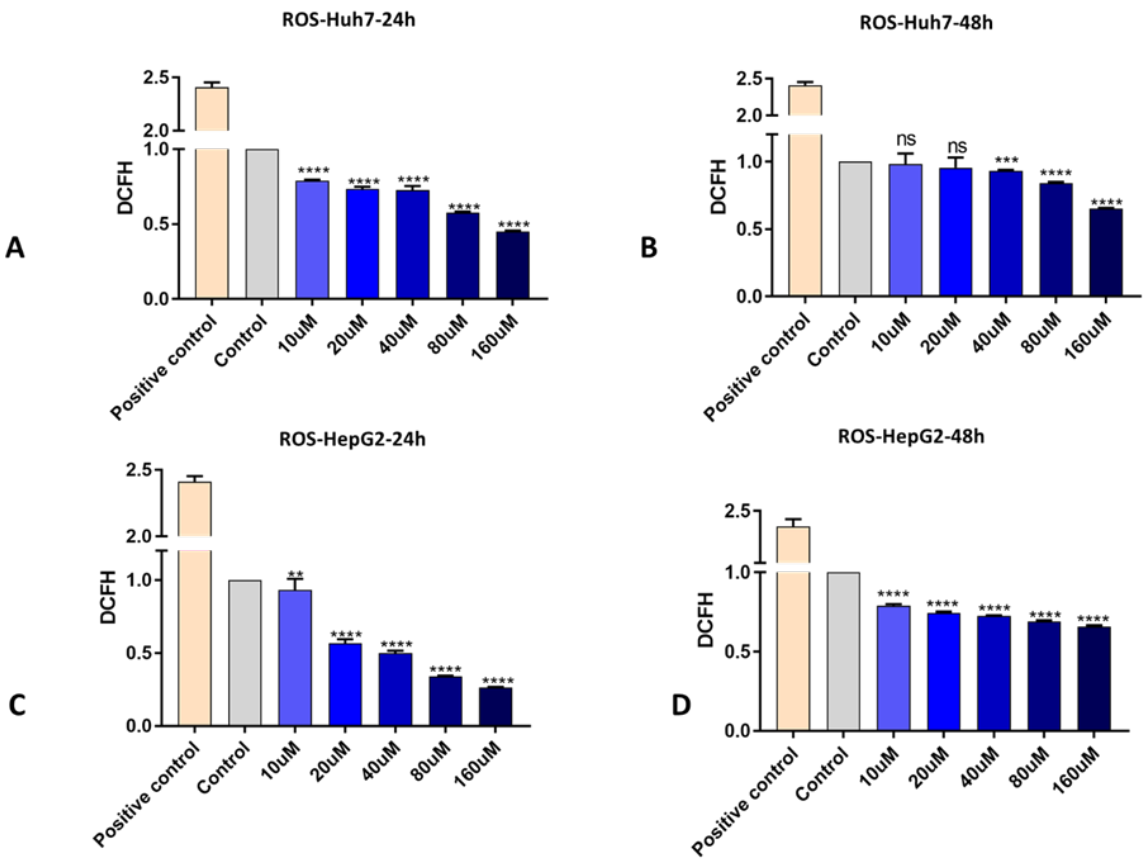

Figure 10: Effect of Tigecycline on ROS levels in HCC cells.

(A) ROS levels of Huh7 after 24 hours and (B) 48 hours of treatment with different concentrations of Tigecycline quantified by DCFH; (C) ROS levels of HepG2 after 24 hours and (D) 48 hours of treatment with different concentrations of Tigecycline; The positive control group is 70% hydrogen peroxide for 1 hour after loading the probes.

DCFH, 2'-7'dichlorofluorescin; ROS, Reactive oxygen species.

3.4 Tigecycline reduces the extend of mitochondrial oxidative phosphorylation (OXPHOS) in HCC cells

To assess the respiratory function of mitochondria in Tigecycline treated cells, mitochondrial oxygen consumption rates (OCR) were analyzed using the Seahorse XFp Analyzer. OCR was significantly decreased after 10 µM Tigecycline treatment in Huh7 cells. The decrease was more pronounced with increasing Tigecycline concentrations (Fig. 11 A).

Further, we analyzed the OCR corresponding to basal respiration, ATP-production and proton leak. Here we also found a significant decrease at 10 µM Tigecycline, with further decrease with increasing Tigecycline concentrations (Fig. 11 C). The same results we obtained in HepG2 cells (Fig. 11 B and D). To assess how Tigecycline treatment affects mitochondrial content, we used Western blot to detect the expression of the respiratory chain subunits Complex I to V. The experimental results showed that low doses of Tigecycline reduce the expression of respiratory chain complexes in both cell lines. However, there is no clear relation to the Tigecycline treatment concentration (Fig. 11 E and F). Also, there is no clear difference between the mtDNA encoded complexes I and IV and the nucDNA encoded complexes II, III and V. Statistical analysis of the relative expression of the respiratory chain subunits in the two cells can be found in Fig. 11 G and H.

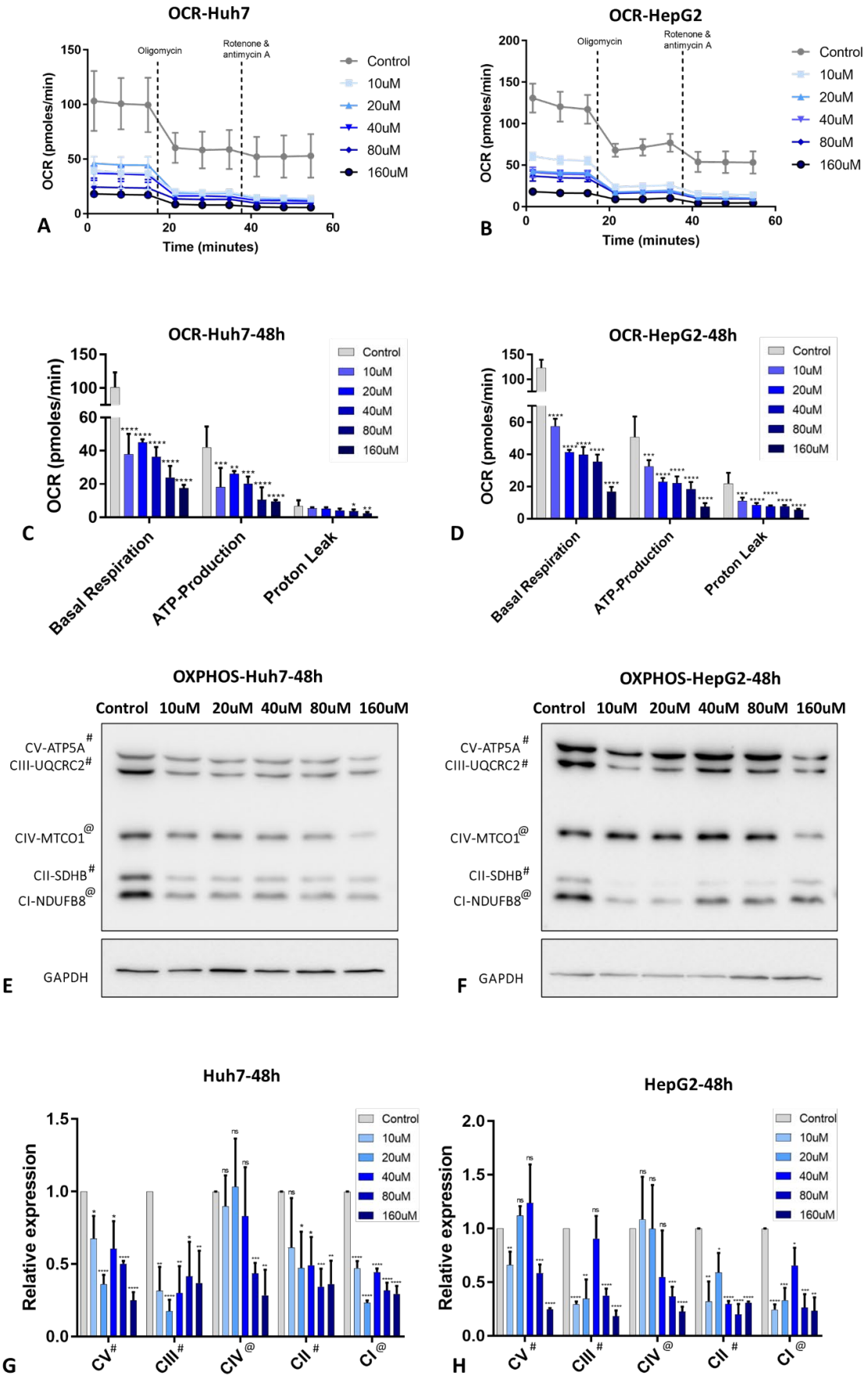
OCR-Huh7
OCR-HepG2
OCR (pmoles/min)
Time (minutes)
Oligomycin
Rotenone & antimycin A
Control
10uM
20uM
40uM
80uM
160uM
A
B
OCR-Huh7-48h
OCR-HepG2-48h
Basal Respiration
ATP-Production
Proton Leak
C
D
OXPHOS-Huh7-48h
OXPHOS-HepG2-48h
CV-ATP5A#
CIII-UQCRC2#
CIV-MTCO1@
CII-SDHB#
CI-NDUFB8@
GAPDH
E
F
Huh7-48h
HepG2-48h
Relative expression
CV#
CIII#
CIV@
CII#
CI@
G
H

Figure 11: Mitochondrial OXPHOS and respiratory chain subunit expression after Tigecycline treatment of HCC cells.

OCR after 48 hours of tigecycline treatment of Huh7 (A) and HepG2 (B) measured by Seahorse XFp Analyzer; Changes in basal respiration, ATP-production and proton leak after different concentrations of Tigecycline treatment in Huh7 (C) and Hep G2 (D); Changes in the expression of the five respiratory chain subunits in Huh7 (E) and HepG2 (F) after Tigecycline treatment assessed by Western blot; (G) and (H) show the statistical analysis of the Western blot images of the expression of the five respiratory chain subunits.

OCR, oxygen consumption rate; CI, Complex I; CII, Complex II; CIII, Complex III; CIV, Complex IV; CV, Complex V. @ means the Complex encoded by the mtDNA; # means the Complex encoded by the nucDNA.

3.5 Tigecycline causes cell cycle change in HCC cells

To further understand the effect of Tigecycline on the growth of HCC cells, we examined the cell cycle changes after Tigecycline treatment of cells using flow cytometry and BrdU. In Huh7, experimental results showed that 10 μM Tigecycline reduced the proportion of cells in S-phase. This percentage decreases with increasing duration of treatment. As the proportion of S-phase cells decreased, the proportion of G0/G1 and G2/M-phase cells increased (Fig. 12 A and C). The same result was reproduced in HepG2 (Fig. 12 B and D).

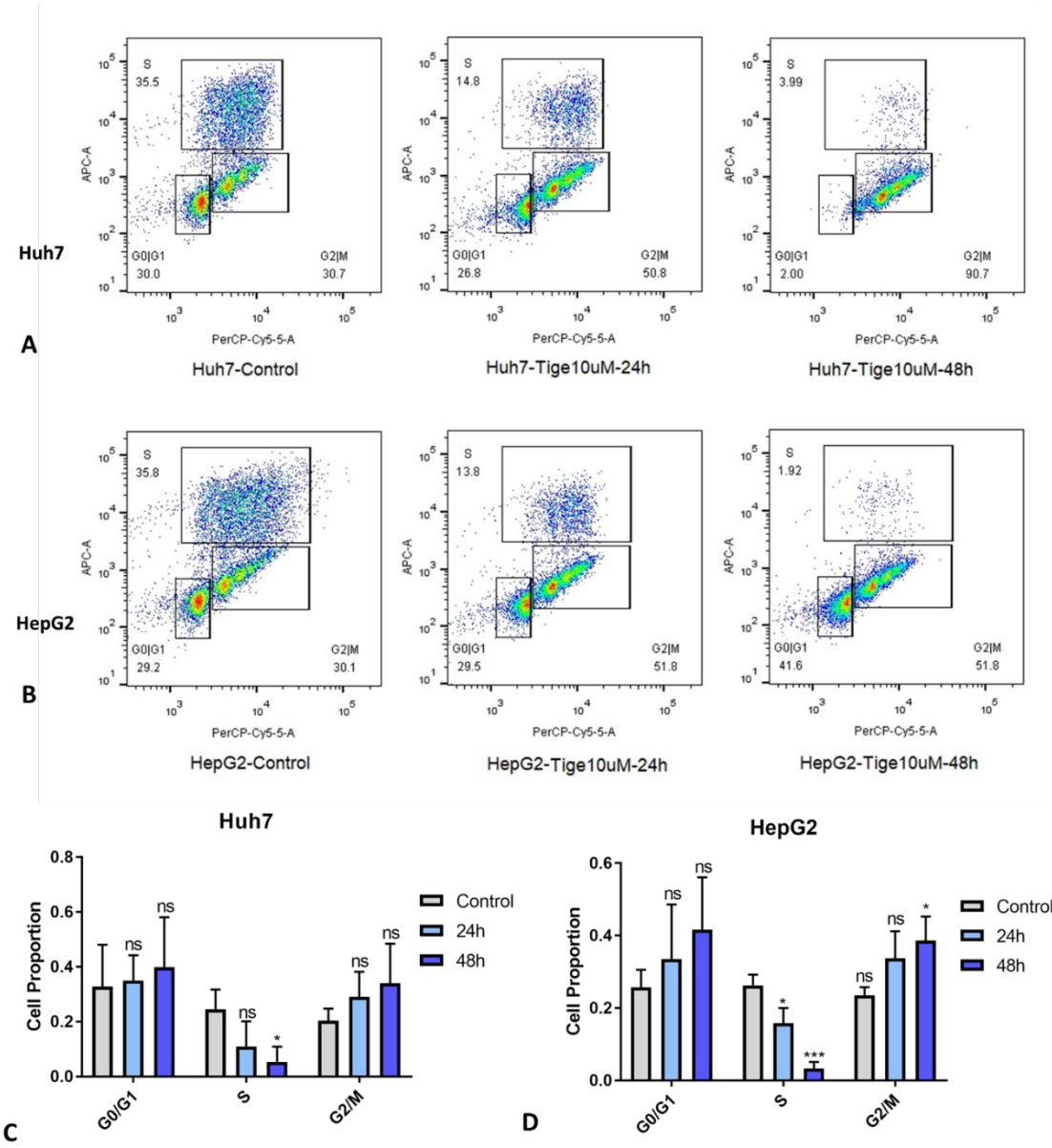

Figure 12: Cell cycle analysis of Tigecycline treated Huh7 and HepG2 cells.

Flow cytometry dot plots showing the changes in the cell cycle of Huh7 (A) and HepG2 (B) after 10 μM tigecycline treatment for 24 hours and 48 hours; Statistical analysis was performed on the percentage of different phases, with results for Huh7 shown in (C) and for HepG2 shown in (D).

3.6 HepG2 and Huh7 are more sensitive to Tigecycline than immortalized hepatocytes

To compare the different effects of Tigecycline on malignant and non-malignant hepatocytes, we used the immortalized normal epithelial liver cell line THLE-2. We treated these immortalized hepatocytes with the same concentration of Tigecycline for 48 hours. The cell viability of the THLE-2 cells decreased with increasing Tigecycline concentration (Fig. 13 A). However, the IC_{50} of THLE-2 with 11.01 µM [$6.419<IC_{50}<18.97$] was higher than that of Huh7 and HepG2, indicating that both hepatocellular carcinoma cells were more susceptible to Tigecycline than the immortalized cell line THLE-2 (IC_{50} Huh7=7.695 µM; IC_{50} HepG2=1.723 µM; IC_{50} THLE-2 = 11.01 µM) (Fig. 13 E). Moreover, the same methods as before were used to detect alterations in ROS and OCR of THLE-2 after treatment with 10 µm and 20 µm of Tigecycline. Comparable to the reaction of the cell lines Huh7 and HepG2, both ROS (Fig. 13 B) and OCR (Fig. 13 C) decreased after Tigecycline treatment of the THLE-2 cell line. At the same time, basal respiration, ATP-production and proton leak were also decreased (Fig. 13 D). Interestingly, we found that THLE-2 showed less decrease in OCR after Tigecycline treatment than Huh7 and HepG2 cells. Flow cytometry was also applied to detect cell cycle changes in THLE-2 after Tigecycline treatment (Fig. 14 A). After repeating the test three times, the results showed that the S-phase of THLE-2 was significantly reduced by 10 µM Tigecycline treatment for 48 hours. However, the cell cycle changes were not as obvious as in the malignant cell lines Huh7 and HepG2 (Fig. 14 C). Similarly, we examined the expression of Complex I to V by Western blot (Fig. 14 B). The results showed that 10 µM and 20 µM Tigecycline decreased the expression of the respiratory chain complexes in THLE-2 cells. The statistical analysis of the relative expression can be found in Fig. 14 D.

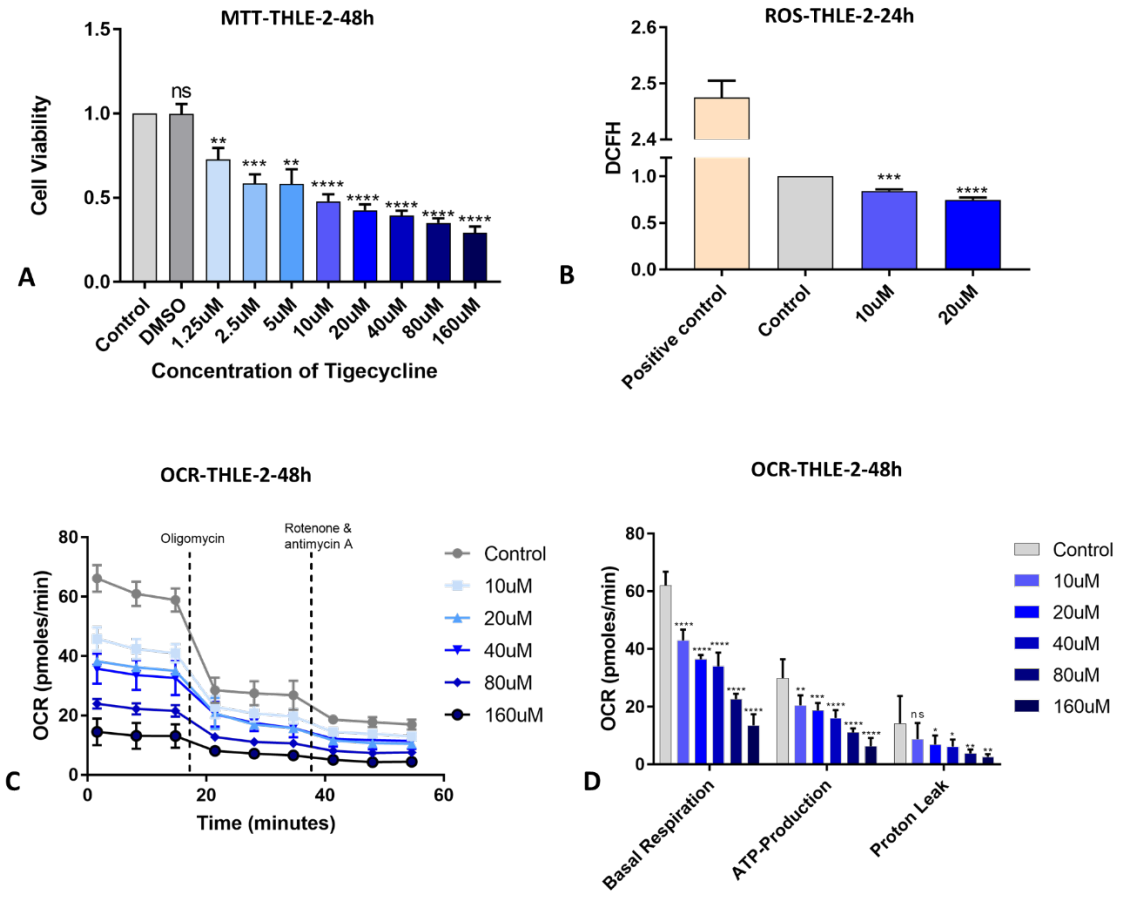

Figure 13: Tigecycline induced cytostatic effect, influence on ROS levels and mitochondrial OXPHOS in non-malignant THLE-2 cells and comparison to the malignant Huh7 and HepG2 cells.

(A) THLE-2 was treated with different concentrations of Tigecycline for 48 hours and cell viability was measured by MTT; (B) ROS levels of THLE-2 after 24 hours of treatment with different concentrations of Tigecycline quantified by DCFH; (C) OCR after 48 hours of Tigecycline treatment of THLE-2 measured by Seahorse XFp Analyzer; (D) Changes in basal respiration, ATP-production and proton leak after different concentrations of Tigecycline treatment of THLE-2 cells;

MTT, 3-(4,5-Dimethylthiazol-2-yl)-2,5-Diphenyltetrazolium Bromide; DCFH, 2'-7'dichlorofluorescin; ROS, reactive oxygen species; OCR, oxygen consumption rate.

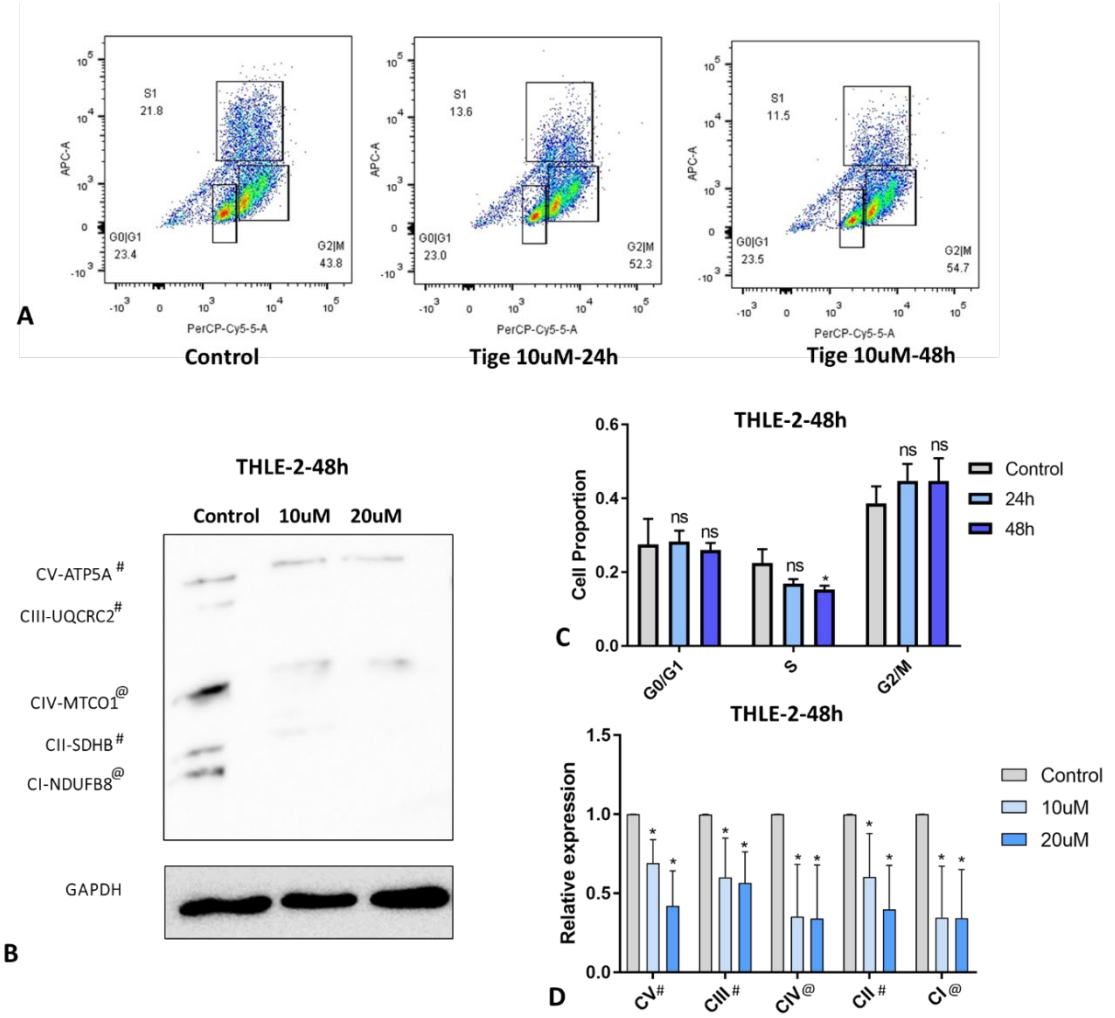

Figure 14: Cell cycle analysis and respiratory chain subunit expressions of Tigecycline treated non-malignant THLE-2 cells

(A) Flow cytometry dot plots showing the changes in the cell cycle THLE-2 cells after 10 μM Tigecycline treatment for 24 hours and 48 hours; (C) Statistical analysis was performed on the percentage of different phases; (B) Changes in the expression of the five respiratory chain subunits in THLE-2 cells after Tigecycline treatment assessed by Western blot; (D) Statistical analysis of the Western blot images of the expression of the five respiratory chain subunits.

CI, Complex I; CII, Complex II; CIII, Complex III; CIV, Complex IV; CV, Complex V. @ means the Complex encoded by the mtDNA; # means the Complex encoded by the nucDNA.

3.7 HepG2 is most sensitive to short-term treatment with Tigecycline regarding OXPHOS

For a typical rapidly proliferating human cell with a total cycle time of 24 hours, the G1-phase might last about 11 hours, S-phase about 8 hours, G2 about 4 hours, and M about 1 hour [97]. Changes in the cell cycle always bring metabolic and energetic changes. We speculate that Tigecycline may interfere with the metabolic cycle of the cells in a much shorter period of time. On the other hand, we have found that both OXPHOS and cell viability were significantly changed after 48 hours of Tigecycline treatment, but the viability of the two cell lines did not change much at 24 hours. Also, it is not clear whether the change in OXPHOS caused the alteration of cell viability or the change in cell viability induced the secondary change in OXPHOS. We are not sure about the causal relationship between the OXPHOS and cytotoxicity. To better understand the causal relationship between the two and the alterations in energy metabolism in the three used cell lines, we shortened the treatment time of Tigecycline to 6 hours. We treated the three cells with 10 μM Tigecycline for 6 hours and then used the Seahorse XFp Analyzer to detect the OCR (Fig. 15 A, C and E) and analyzed basal respiration, ATP-production and proton leak (Fig. 15 B, D and F). We found the greatest change in OCR in HepG2 cells after 10 μM Tigecycline treatment. Also, the basal respiration was significantly reduced in HepG2 (Fig. 15 C and D). By contrast, the immortalized normal hepatocyte cells THLE-2 were not greatly changed (Fig. 15 E and F). To understand the changes in OCR of the three cell lines after a short period of Tigecycline treatment, we analyzed and compared the reduction in basal respiratory OCR after 6 hours of 10 μM Tigecycline treatment (Fig. 15 G). The reduction of HepG2 in basal respiratory OCR was much higher than in the other two cells. THLE-2 seems to be most resistant. The stronger inhibition of mitochondrial OXPHOS of HepG2 by

Tigecycline may be one of the reasons why HepG2 is more sensitive to Tigecycline.

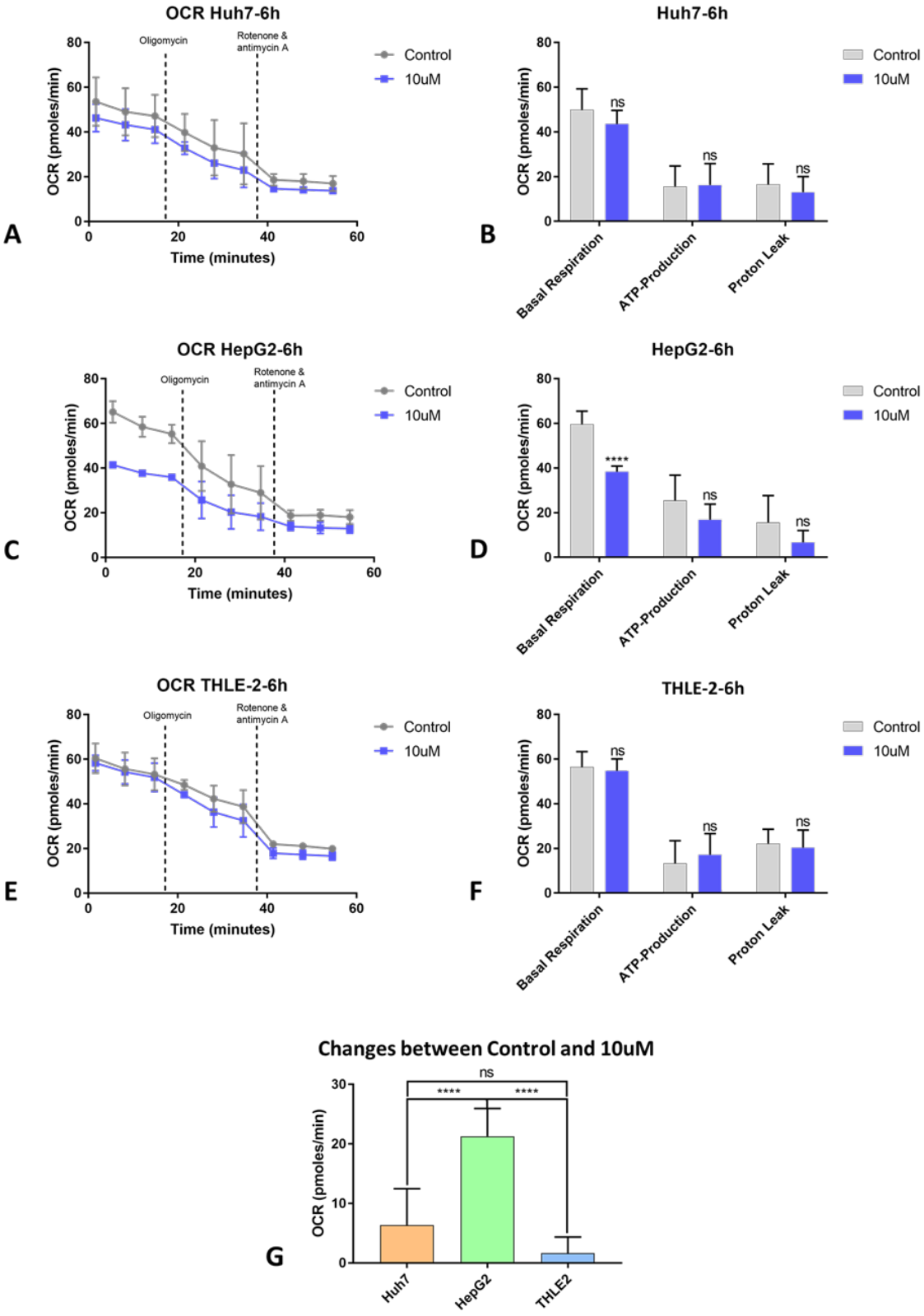

Figure 15: Alterations in mitochondrial OXPHOS after short-term treatment of Huh7, HepG2 and THLE-2.

OCR after 6 hours of 10 µM Tigecycline treatment of Huh7 (A), HepG2 (C) and THLE-2 (E); Changes in basal respiration, ATP-production and proton leak after 10 µM Tigecycline treatment of Huh7 (B), HepG2 (D) and THLE-2 (F); (G) Comparison of the amount of OCR decrease in basal respiration after 10 µM Tigecycline treatment for 6 hours of the malignant cells Huh7 and HepG2 and the non-malignant THLE-2 cells.

3.8 Bioinformatical analysis reveals RAC1 as a potential target for Tigecycline in HCC cells

To identify potential target proteins that mediate the effect of Tigecycline in HCC cells, we conducted a detailed bioinformatical analysis using several established databases. Firstly, we obtained a total of 429 potential genes related to hepatocellular carcinoma from the GeneCards and DisNET databases. In addition, we used the two databases Pharmmaper and Comparative Toxicogenomics Database to identify potential target proteins of Tigecycline and their corresponding genes. We obtained 34 potential target genes for Tigecycline. These 34 potential targets related to Tigecycline and the 429 genes related to HCC were intersected. Thereby we obtained 11 genes that are relevant genes in HCC and code for potential target proteins of Tigecycline (Fig. 16 A). In order to investigate the interaction between the 11 potential genes, STRING 11.5 was used. The results showed that these 11 genes are closely related to each other (Fig. 16 C). KEGG was used to analyze the pathways involved in the 11 genes. KEGG bioinformatics analysis shows that these genes are closely related to inflammation pathways and apoptosis pathways (Fig. 16 D). After differential expression analysis and survival prognosis analysis of these 11 genes using data of The Cancer Genome Atlas Program, we found that only the gene RAC1 was statistically significant in both differential expression (Fig. 16 B, E and F) and survival differences

between tumor and normal tissues (Fig. 16 G and H). Therefore, we propose that RAC1 does play a major role in mediating the effects of Tigecycline in HCC. It may play a role in mediating the growth inhibitory effect of Tigecycline in HCC.

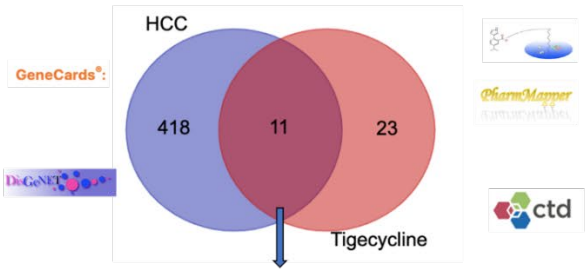

A

DNMT1 CASP3 RAC1 CYCS TNF IL1B
BAD BCL2 SERPINB3 IGF1R IL6

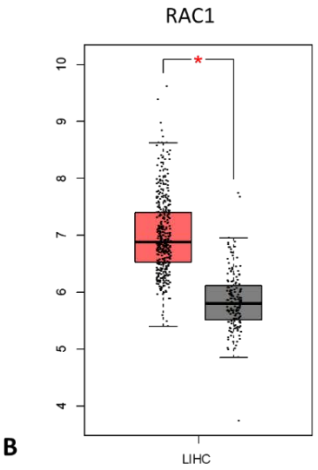

B

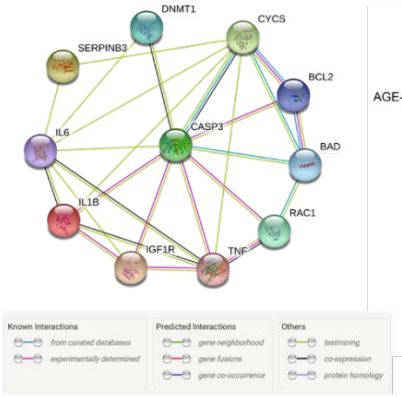

C

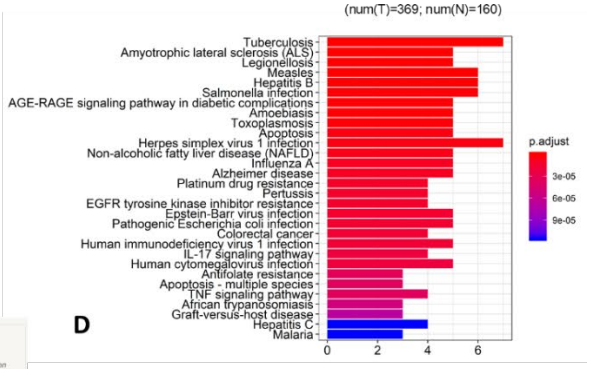

D

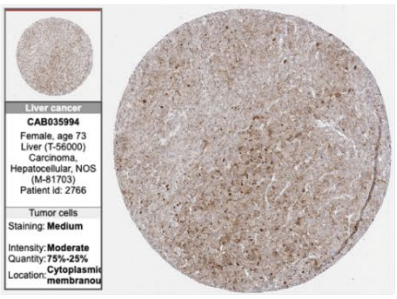

E

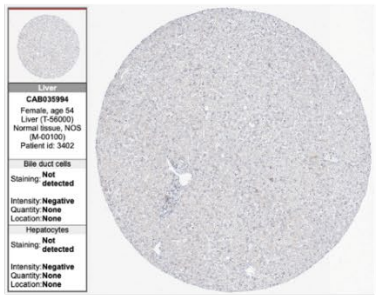

F

RAC1

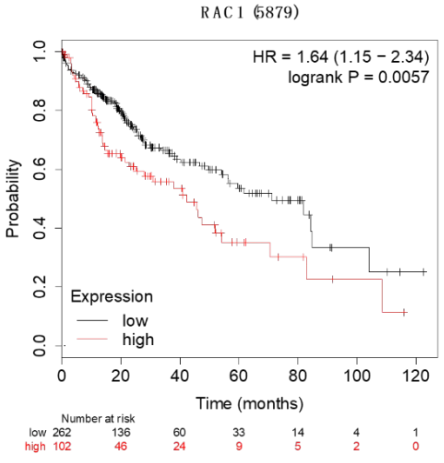

G

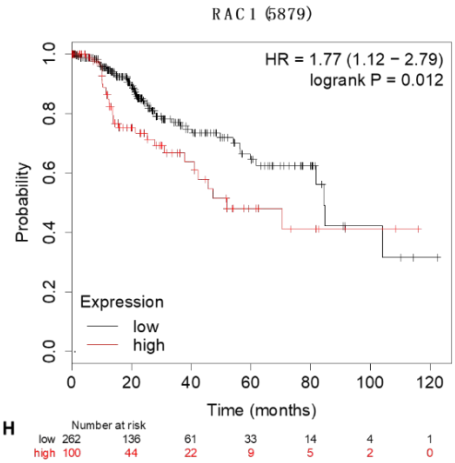

H

Overall Survival (OS)

Disease Free Survival (DSS)

Figure 16: Bioinformatics analysis of Tigecycline and hepatocellular carcinoma.

(A) 429 potential genes related to hepatocellular carcinoma from the GeneCards and DisNET and 34 potential target genes for Tigecycline from Pharmmaper and Comparative Toxicogenomics Database were identified; The intersection reveals 11 relevant genes. (B) The expression of RAC1 in tumors and normal tissues; The data comes from Gepia (http://gepia.cancer-pku.cn/); (C) Protein-protein interaction networks functional enrichment analysis was established with STRING 11.5 (https://string-db.org/); (D) KEGG analysis results of 11 potential genes; The immunohistochemically assessed protein expression of RAC1 in tumor (E) and normal (F) tissues; The data comes from The Human Protein Atlas (https://www.proteinatlas.org/); Survival analysis of OS (G) and DFS (H) of patients with different expression of RAC1; Data comes from Kaplan-Meier plotter (https://kmplot.com/analysis/index.php?p=service&cancer=liver_rnaseq).

LIHC, Liver Hepatocellular Carcinoma; OS, Overall Survial; DFS, Disease Free Survial;

3.9 Tigecycline causes altered RAC1 RNA and protein expression in HCC cells

The G-protein RAC1 was identified as a potential target protein for Tigecycline in HCC. To assess the effects of Tigecycline, we first detected protein expression of RAC1 by Western blot after treatment with different concentrations of Tigecycline for 24 and 48 hours in Huh7. After 24 hours of Tigecycline treatment with 10 µM and 20 µM the protein expression of RAC1 was elevated statistically (Fig. 17 A). In HepG2 the same tendency was seen (Fig. 17 B). To detect the mRNA expression of RAC1 after Tigecycline treatment we used RT-PCR for both HCC cell lines with 10 µM and 20 µM Tigecycline after 24 hours. The results showed that both 10 µM and 20 µM of Tigecycline promoted higher RAC1 mRNA expression in HepG2 and Huh7 (Fig. 17 C). We also compared RAC1 protein and mRNA expression in both cells without Tigecycline treatment, and statistical results showed no

significant difference of RAC1 expression in Huh7 and HepG2 (Fig. 17 D and E).

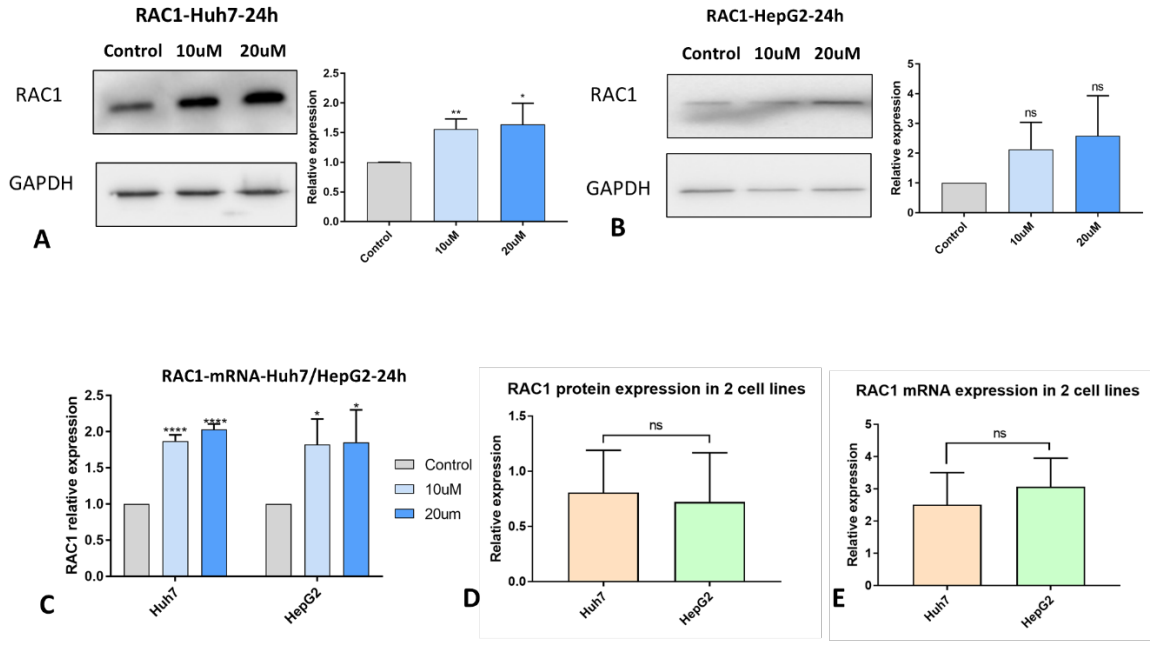

Figure 17: RAC1 mRNA and protein expression of Tigecycline treated HCC cells.

Western blot to detect the protein expression of RAC1 in Huh7 (A) and HepG2 (B) after treatment with 10 μM and 20 μM Tigecycline for 24 hours; (C) RT-PCR to detect the mRNA expression of RAC1 in Huh7 and HepG2 after treatment with 10 μM and 20 μM tigecycline for 24 hours; (D) Western blot to detect the protein expression of RAC1 in Huh7 and HepG2 without any treatment; (E) RT-PCR to detect the mRNA expression of RAC1 in Huh7 and HepG2 without any treatment.

3.10 Tigecycline reduces phosphorylation of ERK1/2

Recently, the latest systematic review on ROS indicated that the reduction of ROS caused by mitochondrial dysfunction would reduce the expression of MAPK/ERK and RAC1 [98]. According to this, we intended to find out which role ERK1/2 plays in hepatocellular carcinoma. Therefore, we used bioinformatics to analyze the expression and prognosis of ERK1 and ERK2 in two cells. ERK1 and ERK2 are highly expressed in liver cancer. Also, patients with high expression of ERK1 and ERK2 have a worse prognosis

(Fig. 18 A, B, D and E). Correlation analysis found that ERK1/2 was positively correlated with RAC1 (Fig. 18 C and F). Western Blot was used to detect the expression of phosphorylated ERK1/2 and ERK1/2 in two cell liness treated with different concentrations of Tigecycline. The results showed that phosphorylated ERK1/2 was reduced, but the total ERK1/2 did not change significantly in Huh7 and HepG2 (Fig. 18 G and J). Fig. 18 H, I, K and L shows the statistical results of three independent experiments. Thereafter, we examined the expression of ERK1/2 and P-ERK1/2 in the two cell lines without any treatment and there was no significant difference between them (Fig. 18 M). So, we speculate that Tigecycline may change the phosphorylation of ERK1/2, but the specific mechanism, especially the connection with RAC1, is still unclear.

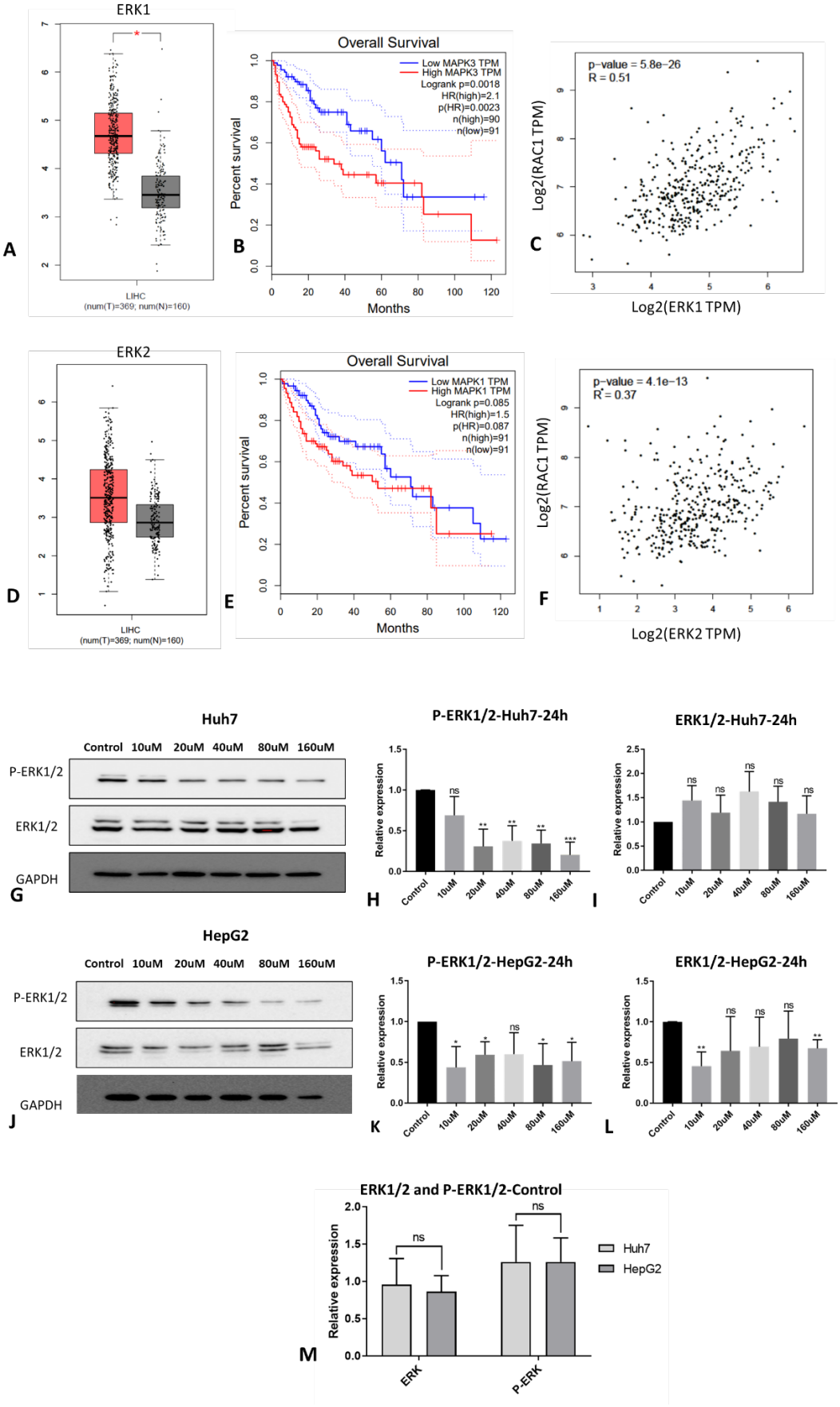

Figure 18: The expression of ERK1/2 in liver cancer and Tigecycline reduces the phosphorylation of ERK1/2.

(A) and (D) The expression of ERK1 and ERK2 in liver cancer is higher than that in normal tissues. (B) and (E) Patients with high expression of ERK1 and ERK2 have a worse prognosis. (C) and (F)The correlation analysis between ERK1 and ERK2 and RAC1 showed a positive correlation. All the data of Fig. 11 A to F come from Gepia (http://gepia.cancer-pku.cn/). (G) and (J) show the Western blot results for the expression of ERK1/2 and p-ERK1/2 in HCC cells. The statistical results of three independent repeated experiments are measured with ImageJ and displayed in (H), (I), (K) and (L). (M) shows Western blot to detect the protein expression of ERK1/2 and p-ERK1/2 in Huh7 and HepG2 without any treatment

3.11 Combination of Tigecycline and Everolimus leads to increased inhibition of HCC cells

Everolimus is a common clinical mTOR receptor inhibitor and does have antitumor effect. It is approved for the treatment of advanced renal cell carcinoma [99]. Moreover, in HCC patients the immunosuppression with Everolimus reduces the HCC recurrence rate after liver transplantation [100, 101]. We compared the effect of Everolimus on the viability of Huh7 and HepG2 cells (Fig. 19 A and B) with the effects of Tigecycline. Here the calculated IC50 values for Everoimus were 7.282 µM [4.865 µM<IC_{50}<11.41 µM] for Huh7 and 12.71 µM [10.49 µM<IC_{50}<15.51 µM] for HepG2. Comparing these IC_{50} values to the Tigecycline IC_{50} values of 7.695 µM [5.703 µM<IC_{50}<10.15 µM] for Huh7 and 1.723 µM [0.953 µM<IC_{50}<2.438 µM] for HepG2 shows comparable values for Huh7 and indicates that Tigecycline is more effective in HepG2.

Furthermore, we did combination experiments. We treated the two HCC cell lines with 10 µM and 20 µM of Tigecycline and Everolimus, respectively, and also treated with 10 µM of Tigecycline and Everolimus in combination. The MTT results showed that the combination of the two drugs reduced the cell viability of the HCC cells more effectively (Fig. 19 C and D).

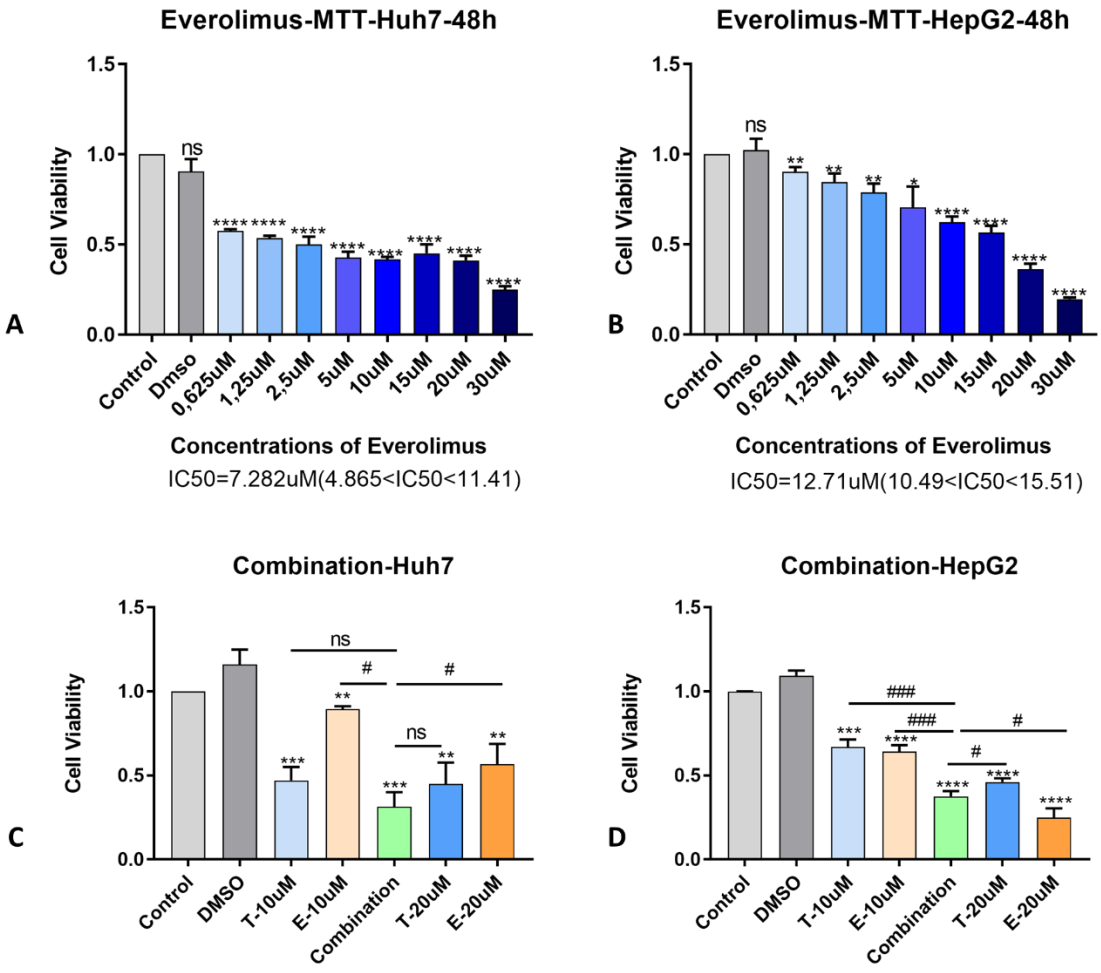

Figure 19: Everolimus induced cytostatic effect on HCC cell lines Huh7 and HepG2 and combination with Tigecycline.

The two cell lines Huh7 (A) and HepG2 (B) were treated with different concentrations of Everolimus for 48 hours and cell viability of both cells was measured by MTT; Huh7 (C) and HepG2 (D) cells were treated with Tigecycline or Everolimus alone and Tigecycline and Everolimus in combination and the cell viability was measured by MTT.

MTT, 3-(4,5-Dimethylthiazol-2-yl)-2,5-Diphenyltetrazolium Bromide; IC_{50}, half maximal inhibitory concentration; T-10 µM, Tigecycline 10 µM; T-20uM, Tigecycline 20 µM; E-10 µM, Everolimus 10 µM; E-20 µM, Everolimus 20 µM; Combination, 10 µM Tigecycline combined with 10 µM Everolimus.

4. Discussion

4.1 The gap between what is known and unknown about Tigecycline

Currently, the treatment of liver cancer is dominated by surgery. Liver transplantation is the most favorable treatment option. However, especially in areas with low organ supply, resection needs to be performed. After resection the recurrence rate of liver cancer remains at a high level. To date, there are no established adjuvant therapy options to improve recurrence rates after resection to gain comparable results like after liver transplantation. Besides new immunotherapies, that are currently tested, we suggest the repurposing of the antibiotic Tigecycline as a new innovative, perioperative and adjuvant therapy strategy.

The Tigecycline has an antibacterial effect because it binds to the 30S ribosomal subunit of bacteria, preventing aminoacyl-tRNA from interacting with the ribosomal A site [75]. Tigecycline has been firstly shown to have anticancer effects in studies of human acute myeloid leukemia, primarily by inhibiting mitochondrial translation [76]. Since then, an increasing number of anticancer studies on Tigecycline have been published.

There are few studies on the effects of Tigecycline on HCC. Tan J et al. discovered in 2017 that Tigecycline increased cisplatin activity against hepatocellular carcinoma by generating mitochondrial dysfunction and oxidative damage [80]. Recent studies have also found that Tigecycline could be considered as a second-line treatment when HCC patients are resistant to Sorafenib [102]. Other than that, no further basis studies on Tigecycline and HCC can be found. Moreover, the existing studies never directly focused on potential target proteins of Tigecycline in HCC. Also, the effect of Tigecycline on normal hepatocytes have never been focused in detail. On this basis we have carried out our research.

4.2 Our findings

Our study firstly reported that Tigecycline inhibits growth of the two different HCC cell lines Huh7 and HepG2. Interestingly, the IC_{50} of the two cell lines differs significantly. HepG2 is more sensitive to Tigecycline than Huh7. To better simulate tumor growth environment and stem cell characteristics, we used sphere formation assays as a three-dimensional culture model. The cell line Huh7 was more sensitive than HepG2 in this three-dimensional culture model. In addition, we found that both invasion and migration were inhibited significantly by Tigecycline.

To search for mechanisms, we examined changes in OXPHOS and ROS production in both types of cells after Tigecycline treatment. Changes in the cell cycle were also focused on. To fill a gap in the research on the effects of Tigecycline on normal hepatocytes, we repeated all of the above mentioned experiments with the immortalized normal hepatocyte cell line THLE-2.

In addition, to search for potential target proteins of Tigecycline action in HCC, we used detailed bioinformatics analysis. We identified RAC1 as a potential target gene and analyzed the changes in RAC1 in response to Tigecycline treatment. Eventually, in order to explore new clinical applications, we tested the combination of Everolimus and Tigecycline, and obtained good anticancer results.

4.3 Differences in the sensitivity of Tigecycline in three cell lines

In the initial stages of our experiment, we found a significant difference in the sensitivity of HepG2 and Huh7 to Tigecycline. We consider that this may be due to the heterogeneity of the different cells. Back in 2018, Jian S et al. performed a principal component analysis of the expression profiles of 101 drug-metabolizing enzymes data of Hep3B, HepG2 and Huh7 cell lines. The

research revealed that Hep3B and Huh7 had extremely comparable drug-metabolizing enzyme expression patterns, however, HepG2 diverged greatly from them [103]. This finding might be related to the diverse origins of these cells. HepG2 was generated from newborn liver stem cells taken from a hepatoblastoma liver biopsy sample [104], which may have greater differential potential, whereas Hep3B and Huh7 were obtained from highly differentiated HCC cells. [105-107]. A further discrepancy in the sensitivity to Tigecycline is seen with the cell line THLE-2, which is an immortalized hepatocyte cell line. Our results show that THLE-2 has a higher IC_{50} value (11.01 μM) than both tested HCC cell lines. This is an encouraging result and means that Tigecycline could kill tumor cells with limited damage to normal hepatocytes as long as the dose is well controlled. In the course of our studies, we found that the biggest difference between THLE-2 and HCC cell lines is in terms of OXPHOS of mitochondria. They all reduced their OCR as a result of Tigecycline treatment, but at the same concentration, THLE-2 showed the least change in OCR. THLE-2 tolerance to Tigecycline-induced alterations in mitochondrial OXPHOS may have occurred earlier than we thought. In our short-term experiment of 6h Tigecycline treatment, the OCR of THLE-2 did not change significantly. In contrast, the reduction of OCR in HepG2 is much higher than THLE-2 and Huh7. As mentioned above, this may be caused by different drug-metabolizing enzymes. We can rationally speculate that because of the difference in drug-metabolizing enzymes makes HepG2 has different energy requirements. Tigecycline does have strong effect to the inhibition of OXPHOS metabolism of HepG2, resulting in a large reduction of energy production within HepG2 with a low dose of Tigecycline. Furthermore, cells that lack energy cannot perform DNA synthesis which leads to growth inhibition or even death.

4.4 Causal relationship between cytotoxicity and OXPHOS

In our experimental results, we found that Tigecycline had an inhibitory effect on all cells at 48 hours, reducing the viability of the cells and exhibiting cytotoxicity. Also, the negative effect of Tigecycline on mitochondrial OXPHOS was shown in our 48 hours experimental results. But what is the sequence in which these two changes occur? And what is the causal relationship between these two changes? It is well documented that alterations in OXPHOS can modify the cytotoxicity of resveratrol, which is related to energy metabolism [108]. However, we cannot exclude the possibility that increased cytotoxicity directly causes cell death, and then OXPHOS decreases subsequently. Therefore, in our experimental design, the time of Tigecycline treatment of three cells was shortened to 6 hours, and then OXPHOS was detected. Our experimental results showed that the inhibitory effect of Tigecycline on OXPHOS had been produced at 6 hours. However, there was no significant change in cell viability in the MTT results even at 24h. So, we can assume that the change of OXPHOS precedes the change of cell viability. This also confirms our speculation that the negative effect of Tigecycline on OXPHOS enhances the cytotoxicity of Tigecycline causing a decrease in cell viability.

4.5 The role of RAC1 in tumors: friend or foe?

Rac family small GTPase 1 (RAC1) encodes a GTPase that belongs to the RAS superfamily of small GTP-binding proteins. Members of RAC family play different roles in a variety of cellular functions, including control of cytoskeletal re-organization, activation of protein kinases, and cell growth and proliferation [109, 110]. Rac1 may also play a role in cell invasion and migration. There are articles reporting that RAC1 can control the cell contraction and membrane protrusion, which all affect cell invasion and migration [111]. RAC1 is prone to mutation in a range of cells, with a prominent

hotspot at P29. The number of mutations is increased in uterine cancer, melanoma, and HNSCC [112, 113]. These mutations enhance the activity of Rac1, but do not prevent it from circulating between the GTP and GDP bound form. A deletion of the Rac1 gene in the lung or pancreas significantly reduced tumor formation in those organs, indicating that Rac1 activation is critical in a variety of cancers [114, 115]. Likewise, overexpression of RAC1 has been linked to a number of cancer cell phenotypes associated with tumor development, metastasis, treatment resistance and a poor prognosis for patients with a range of solid tumors [116-118].

As mentioned before, the signaling of RAC1 is involved in several biological processes in cells. RAC1 is a small GTPase that alternates between active and inactive states [109]. Such variations occur mainly in some subcellular locations including mitochondria, nucleus, and cytoplasmic membrane. However, it is known that the pathways and biological functions of RAC1 in different locations are very different.

As early as 1991, RAC1 was found to regulate the phagocytosis of the plasma membrane [119]. At the plasma membrane, RAC1 interacts with guanine nucleotide exchange factors (GEFs), receptor tyrosine kinases (RTKs), adhesion molecules and scaffolding proteins [120]. RAC1 has also been linked to the formation and location of macrophage tunneling nanotubes (TNTs), which are membranous channels that connect cells and may transport a variety of signaling chemicals such as vesicles and organelles [121]. To summarize briefly, RAC1 cannot become a transmembrane protein due to its hydrophilic structure, but it can bind to phospholipids and adhesion proteins. Such interactions, in turn, can also change the biological functions of the plasma membrane.

There is much less studied about RAC1 in the nucleus than on the plasma membrane. The existence of nuclear RAC1 was discovered in recent studies [122]. The nuclear location of RAC1 depends on the cell cycle. At the end of G2-phase, nuclear localization increased while at the beginning of G1-phase there is nuclear exclusion [123]. In the G2-phase, RAC1 was also found to be involved in the process of centrosome separation [124]. Recently, TIAM1, a guanine nucleotide exchange factor specific for RAC1, was

discovered to negatively regulate the transcriptional activity of YAP/TAZ in the nucleus of gastrointestinal tumor cells, reducing their invasiveness [125]. In addition, studies have shown that DNA damage and inflammation mediated by Rac1 promote Nf2 tumorigenesis. The main mechanism is the regulation of the Hippo-Yap and Rac1-Pak1 pathways [126].

Compared with the previous two subcellular locations, we pay more attention to the locations and function of RAC1 on the mitochondria. The mitochondrial localization of RAC1 is the latest subcellular localization that was discovered. The first discovery of mitochondrial RAC1 was in B cell lymphoma cells with BCL2 overexpressing [127]. The main function of mitochondrial RAC1 is to mediate the production of superoxide, which can have cytoprotective or cytotoxic effects. The impact of this "two-edged sword" is determined by cell type and environmental factors such as glycolysis and other metabolic levels [128, 129]. In addition, RAC1 is also involved in the electron transport of the respiratory chain on the mitochondria [130].

As described, we initially identified 11 potential genes that are relevant genes in HCC and code for potential target proteins of Tigecycline, but only RAC1 of these 11 potential genes differed in expression and survival analysis. So, we chose RAC1 to continue our study. According to bioinformatic findings, RAC1 is highly expressed in cancer and that high expression is associated with a poor prognosis. Numerous basic studies have also shown that reduced RAC1 expression exhibits inhibition of hepatocellular carcinoma [131-134]. Interestingly, we have repeatedly confirmed increased expression of RAC1 in response to Tigecycline stimulation with RT-PCR at mRNA and Western blot at protein level. For the first time, we found that Tigecycline increased the expression of RAC1 when it inhibited cell viability, which is a very interesting phenomenon. It is possible that there are other pathways that activate RAC1 expression and also kill tumor cells.

However, analyzing the total amount of RAC1 mRNA and protein expression is limited. In fact, RAC1 is distributed in different subcellular organelles, such as mitochondrial RAC1, nuclear RAC1, and plasma membrane

RAC1[135]. These different distributions of RAC1 may have different biological functions. Moreover, RAC1 can be modified by phosphorylation and the RAC1 activation could be assessed on top. After we found that RAC1 is altered in Huh7 and HepG2, we wondered whether RAC1 changes in THLE-2 cells and whether such differences are responsible for their differential sensitivity to Tigecycline. Unfortunately, we did not get any results when we used Western blot to detect the expression of RAC1 in THLE-2. Combined with the bioinformatics data, we believe that this may be due to the low expression of RAC1 in normal tissues or cells.

4.6 Relationship between RAC1 and ROS

A large amount of literature suggests an inextricable relationship between RAC1 and ROS. Few papers have been able to clearly elucidate the relationship between RAC1 and ROS. Some articles suggest that changes in RAC1 are a prerequisite for changes in ROS [136-139]. Some articles also suggest that changes in ROS affect the activity of RAC1 [140, 141]. There is not much literature on the relationship between Tigecycline and ROS. However, several of these articles suggest that Tigecycline increases the production of ROS [80, 81, 142]. This was contrary to the results of our experiments which were repeated several times. We evaluated the formation of ROS in all three cell lines using H_2O_2 as a positive control and found that there was a decrease after 24 hours in all cases. However, our observed inhibition of mitochondrial function by Tigecycline is supported by other studies [143]. Nolfi-Donegan et al. clearly described the relationship between mitochondrial function and ROS in a review, accordingly we suggest that the reduction in ROS may be related to the inhibition of mitochondrial OXPHOS [144].

In addition, the latest systematic review on ROS indicated that the reduction of ROS caused by mitochondrial dysfunction would reduce the expression

of MAPK/ERK and RAC1 [98]. Therefore, we used bioinformatics to analyze the expression and prognosis of ERK1 and ERK2. Correlation analysis found that ERK1/2 was positively correlated with RAC1. The expression of phosphorylated ERK1/2 and ERK1/2 was detected by Western blot in two cells treated with various doses of Tigecycline. The results indicated that phosphorylated ERK1/2 were decreased, while overall ERK1/2 remained unchanged. So, we speculate that Tigecycline may change the phosphorylation of ERK1/2, but the explicit mechanism, especially the connection with RAC1, is still unclear. This is also the direction we want to study next.

4.7 Tigecycline and cell cycle

The cell cycle is closely related to tumor growth and metabolism, and its regulation can be a promising target for cancer therapy [145, 146]. Numerous studies have demonstrated that Tigecycline arrests the cell cycle in the G0/G1-phase in a variety of malignancies, including melanoma [88], glioma [83], and pancreatic ductal adenocarcinoma [147]. These studies have generally considered that a reduction in cyclin D1 and CDK family members (CDK2 and CDK4) is associated with cell cycle arrest. Some studies also hold a different view, with Bo Hu and Yue Guo in a study of ovarian cancer suggesting that Tigecycline causes cell cycle arrest in the G2/M-phase instead of the G0/G1-phase [86]. Interestingly, our results are different from any previous study. For the first time, we found that the cell cycle of the Tigecycline arrest in HCC is in the S phase instead of G0/G1 and G2/M-phases. We found reasonable support in the literature to explain this phenomenon. DNA synthesis occurs during the S-phase and it is possible that Tigecycline interferes with DNA synthesis. In plant and animal cells, the beginning and termination of DNA synthesis, as well as mitosis, are energy-dependent and need OXPHOS [148, 149]. According to reports, aerobic glycolysis peaks when lymphocytes enter the S-phase [150, 151]. Based on our

previous description, we speculate that the S-phase is arrested because of the lack of a large energy supply. The S-phase arrest occurs because of the reduced supply of energy for DNA synthesis due to the Tigecycline induced weakening of mitochondrial OXPHOS.

4.8 Exploration of Tigecycline combination

Drug resistance in tumor cells is a major obstacle in cancer treatment [152]. Tigecycline in association with numerous chemotherapeutic agents may improve the responsiveness of certain hematological malignancies and solid tumors to chemotherapy. Tigecycline has synergistic effects with cisplatin in ovarian cancer [86] and HCC [80]. Furthermore, Tigecycline in combination with paclitaxel dramatically improved the in vitro and in vivo therapy of renal cell cancer [153]. In hematological malignancies, the combination of Tigecycline with doxorubicin and vincristine has a synergistic effect in acute lymphoblastic leukemia [84]. In Myc-driven lymphomas [154], Tigecycline exhibits significant apoptosis because it interferes with the function of mitochondria. Meanwhile, a preclinical study showed that Tigecycline and venetoclax synergistically inhibited MYC/BCL-2 double-hit B cell lymphomas [155]. Everolimus, an inhibitor of the mTOR receptor inhibitor, is now licensed for treatment in patients with late kidney cancer who have failed conventional therapy [156], and was approved by the FDA in July 2012 for a treat in conjunction with exemestane in patients with ER+, HER2- breast cancer [157]. Everolimus is also used in the prevention of organ rejection after liver transplantation [158] and results in reduced recurrence rates after liver transplantation of HCC patients [100, 101]. Despite the recognized role of Everolimus in the prevention of organ rejection and in the reduction of HCC recurrence rates after liver transplantation, patients with non-resected HCC do not benefit from a systemic therapy with Everolimus [159]. Whether the combination of Everolimus and Tigecycline has a synergistic effect in

HCC raised our curiosity. So, we performed experiments in HepG2 and Huh7 cells with the combination of the two drugs. The results of the in vitro experiment are promising, but whether it can be applied to the clinic still needs to wait for more data to support this.

5. Conclusion

In conclusion, our study investigated the promising inhibitory effect of Tigecycline on HCC. Moreover, the role of RAC1 in the mechanism of inhibition was explored for the first time. Also, we found some different findings from previous studies, such as Tigecycline decreased ROS production and Tigecycline induced cell cycle arrest in S-phase instead of G0/G1 and G2/M-phase. Most importantly, we also studied the influence of Tigecycline on normal hepatocytes and revealed differential reaction which indicate that Tigecycline could kill tumor cells with limited damage to normal hepatocytes as long as the dose is well controlled.

6. References

[1] H. Sung *et al.*, "Global Cancer Statistics 2020: GLOBOCAN Estimates of Incidence and Mortality Worldwide for 36 Cancers in 185 Countries," *CA Cancer J Clin,* vol. 71, no. 3, pp. 209-249, May 2021, doi: 10.3322/caac.21660.

[2] A. Forner, M. Reig, and J. Bruix, "Hepatocellular carcinoma," *Lancet,* vol. 391, no. 10127, pp. 1301-1314, Mar 31 2018, doi: 10.1016/S0140-6736(18)30010-2.

[3] A. Tang, O. Hallouch, V. Chernyak, A. Kamaya, and C. B. Sirlin, "Epidemiology of hepatocellular carcinoma: target population for surveillance and diagnosis," *Abdom Radiol (NY),* vol. 43, no. 1, pp. 13-25, Jan 2018, doi: 10.1007/s00261-017-1209-1.

[4] A. Jemal *et al.*, "Annual Report to the Nation on the Status of Cancer, 1975-2014, Featuring Survival," *J Natl Cancer Inst,* vol. 109, no. 9, Sep 1 2017, doi: 10.1093/jnci/djx030.

[5] M. Arnold *et al.*, "Global Burden of 5 Major Types of Gastrointestinal Cancer," *Gastroenterology,* vol. 159, no. 1, pp. 335-349 e15, Jul 2020, doi: 10.1053/j.gastro.2020.02.068.

[6] S. A. Khan, H. C. Thomas, B. R. Davidson, and S. D. Taylor-Robinson, "Cholangiocarcinoma," *Lancet,* vol. 366, no. 9493, pp. 1303-14, Oct 8 2005, doi: 10.1016/S0140-6736(05)67530-7.

[7] J. D. Yang, P. Hainaut, G. J. Gores, A. Amadou, A. Plymoth, and L. R. Roberts, "A global view of hepatocellular carcinoma: trends, risk, prevention and management," *Nat Rev Gastroenterol Hepatol,* vol. 16, no. 10, pp. 589-604, Oct 2019, doi: 10.1038/s41575-019-0186-y.

[8] J. L. Petrick *et al.*, "International trends in hepatocellular carcinoma incidence, 1978-2012," *Int J Cancer,* vol. 147, no. 2, pp. 317-330, Jul 15 2020, doi: 10.1002/ijc.32723.

[9] A. A. Florio *et al.*, "Global trends in intrahepatic and extrahepatic cholangiocarcinoma incidence from 1993 to 2012," *Cancer,* vol. 126, no. 11, pp. 2666-2678, Jun 1 2020, doi: 10.1002/cncr.32803.

[10] J. L. Petrick and K. A. McGlynn, "The changing epidemiology of primary liver cancer," *Curr Epidemiol Rep,* vol. 6, no. 2, pp. 104-111, Jun 2019, doi: 10.1007/s40471-019-00188-3.

[11] N. C. D. R. F. Collaboration, "Worldwide trends in diabetes since 1980: a pooled analysis of 751 population-based studies with 4.4 million participants," *Lancet,* vol. 387, no. 10027, pp. 1513-1530, Apr 9 2016, doi: 10.1016/S0140-6736(16)00618-8.

[12] N. C. D. R. F. Collaboration, "Trends in adult body-mass index in 200 countries from 1975 to 2014: a pooled analysis of 1698 population-based measurement studies with 19.2 million participants," *Lancet,* vol. 387, no. 10026, pp. 1377-1396, Apr 2 2016, doi: 10.1016/S0140-6736(16)30054-X.

[13] K. D. Miller, M. Fidler-Benaoudia, T. H. Keegan, H. S. Hipp, A. Jemal, and R. L. Siegel, "Cancer statistics for adolescents and young adults, 2020," *CA Cancer J Clin,* vol. 70, no. 6, pp. 443-459, Nov 2020, doi: 10.3322/caac.21637.

[14] L. European Association For The Study Of The, R. European Organisation For, and C. Treatment Of, "EASL-EORTC clinical practice guidelines: management of hepatocellular carcinoma," *J Hepatol,* vol. 56, no. 4, pp. 908-43, Apr 2012, doi: 10.1016/j.jhep.2011.12.001.

[15] R. J. Aragon and N. L. Solomon, "Techniques of hepatic resection," *J Gastrointest Oncol,* vol. 3, no. 1, pp. 28-40, Mar 2012, doi: 10.3978/j.issn.2078-6891.2012.006.

[16] T. Wakai *et al.*, "Anatomic resection independently improves long-term survival in patients with T1-T2 hepatocellular carcinoma," *Ann Surg Oncol,* vol. 14, no. 4, pp. 1356-65, Apr 2007, doi: 10.1245/s10434-006-9318-z.

[17] J. Chen *et al.*, "The safety and efficacy of laparoscopic and open hepatectomy in hepatocellular carcinoma patients with liver cirrhosis: a systematic review," *Int J Clin Exp Med,* vol. 8, no. 11, pp. 20679-89, 2015. [Online]. Available: https://www.ncbi.nlm.nih.gov/pubmed/26884991.

[18] G. B. Levi Sandri *et al.*, "Laparoscopic and robotic approach for hepatocellular carcinoma-state of the art," *Hepatobiliary Surg Nutr,* vol. 5, no. 6, pp. 478-484, Dec 2016, doi: 10.21037/hbsn.2016.05.05.

[19] A. Khandoga *et al.*, "Differential significance of early surgical complications for acute and long-term recurrence-free survival following surgical resection of hepatocellular carcinoma: do comorbidities play a role?," *Eur J Gastroenterol Hepatol,* vol. 29, no. 9, pp. 1045-1053, Sep 2017, doi: 10.1097/MEG.0000000000000912.

[20] M. B. Schoenberg *et al.*, "Development of novel biological resection criteria for safe and oncologically satisfying resection of hepatocellular carcinoma," *Surg Oncol,* vol. 27, no. 4, pp. 663-673, Dec 2018, doi: 10.1016/j.suronc.2018.08.007.

[21] J. M. Llovet *et al.*, "Cost effectiveness of adjuvant therapy for hepatocellular carcinoma during the waiting list for liver transplantation," *Gut,* vol. 50, no. 1, pp. 123-8, Jan 2002, doi: 10.1136/gut.50.1.123.

[22] J. Bruix, M. Sherman, and D. American Association for the Study of Liver, "Management of hepatocellular carcinoma: an update," *Hepatology,* vol. 53, no. 3, pp. 1020-2, Mar 2011, doi: 10.1002/hep.24199.

[23] J. Belghiti and R. Kianmanesh, "Surgical treatment of hepatocellular carcinoma," *HPB (Oxford),* vol. 7, no. 1, pp. 42-9, 2005, doi: 10.1080/13651820410024067.

[24] J. M. Llovet *et al.*, "Sorafenib in advanced hepatocellular carcinoma," *N Engl J Med,* vol. 359, no. 4, pp. 378-90, Jul 24 2008, doi: 10.1056/NEJMoa0708857.

[25] A. L. Cheng *et al.*, "Efficacy and safety of sorafenib in patients in the Asia-Pacific region with advanced hepatocellular carcinoma: a phase III randomised, double-blind, placebo-controlled trial," *Lancet Oncol,* vol. 10, no. 1, pp. 25-34, Jan 2009, doi: 10.1016/S1470-2045(08)70285-7.

[26] J. M. Llovet, A. Villanueva, A. Lachenmayer, and R. S. Finn, "Advances in targeted therapies for hepatocellular carcinoma in the genomic era," *Nat Rev Clin Oncol,* vol. 12, no. 7, pp. 408-24, Jul 2015, doi: 10.1038/nrclinonc.2015.103.

[27] C. Akateh *et al.*, "Neoadjuvant and adjuvant treatment strategies for hepatocellular carcinoma," *World J Gastroenterol,* vol. 25, no. 28, pp. 3704-3721, Jul 28 2019, doi: 10.3748/wjg.v25.i28.3704.

[28] Q. Xiang *et al.*, "Cabozantinib suppresses tumor growth and metastasis in hepatocellular carcinoma by a dual blockade of VEGFR2 and MET," *Clin Cancer Res,* vol. 20, no. 11, pp. 2959-70, Jun 1 2014, doi: 10.1158/1078-0432.CCR-13-2620.

[29] J. Bruix, K. H. Han, G. Gores, J. M. Llovet, and V. Mazzaferro, "Liver cancer: Approaching a personalized care," *J Hepatol,* vol. 62, no. 1 Suppl, pp. S144-56, Apr 2015, doi: 10.1016/j.jhep.2015.02.007.

[30] J. M. Llovet, C. Bru, and J. Bruix, "Prognosis of hepatocellular carcinoma: the BCLC staging classification," *Semin Liver Dis,* vol. 19, no. 3, pp. 329-38, 1999, doi: 10.1055/s-2007-1007122.

[31] S. Shiina *et al.*, "Radiofrequency ablation for hepatocellular carcinoma: 10-year outcome and prognostic factors," *Am J Gastroenterol,* vol. 107, no. 4, pp. 569-77; quiz 578, Apr 2012, doi: 10.1038/ajg.2011.425.

[32] S. K. Yeo and J. L. Guan, "Breast Cancer: Multiple Subtypes within a Tumor?," *Trends Cancer,* vol. 3, no. 11, pp. 753-760, Nov 2017, doi: 10.1016/j.trecan.2017.09.001.

[33] K. Schulze, J. C. Nault, and A. Villanueva, "Genetic profiling of hepatocellular carcinoma using next-generation sequencing," *J Hepatol,* vol. 65, no. 5, pp. 1031-1042, Nov 2016, doi: 10.1016/j.jhep.2016.05.035.

[34] J. M. Llovet *et al.*, "Hepatocellular carcinoma," *Nat Rev Dis Primers,* vol. 2, p. 16018, Apr 14 2016, doi: 10.1038/nrdp.2016.18.

[35] J. Zucman-Rossi, A. Villanueva, J. C. Nault, and J. M. Llovet, "Genetic Landscape and Biomarkers of Hepatocellular Carcinoma," *Gastroenterology,* vol. 149, no. 5, pp. 1226-1239 e4, Oct 2015, doi: 10.1053/j.gastro.2015.05.061.

[36] I. Martinez-Quetglas *et al.*, "IGF2 Is Up-regulated by Epigenetic Mechanisms in Hepatocellular Carcinomas and Is an Actionable Oncogene Product in Experimental Models," *Gastroenterology,* vol. 151, no. 6, pp. 1192-1205, Dec 2016, doi: 10.1053/j.gastro.2016.09.001.

[37] Y. Wu, Y. Zhang, X. Qin, H. Geng, D. Zuo, and Q. Zhao, "PI3K/AKT/mTOR pathway-related long non-coding RNAs: roles and mechanisms in hepatocellular carcinoma," *Pharmacol Res,* vol. 160, p. 105195, Oct 2020, doi: 10.1016/j.phrs.2020.105195.

[38] B. Delire and P. Starkel, "The Ras/MAPK pathway and hepatocarcinoma: pathogenesis and therapeutic implications," *Eur J Clin Invest,* vol. 45, no. 6, pp. 609-23, Jun 2015, doi: 10.1111/eci.12441.

[39] S. Xia, Y. Pan, Y. Liang, J. Xu, and X. Cai, "The microenvironmental and metabolic aspects of sorafenib resistance in hepatocellular carcinoma," *EBioMedicine,* vol. 51, p. 102610, Jan 2020, doi: 10.1016/j.ebiom.2019.102610.

[40] A. Villanueva *et al.*, "Notch signaling is activated in human hepatocellular carcinoma and induces tumor formation in mice," *Gastroenterology,* vol. 143, no. 6, pp. 1660-1669 e7, Dec 2012, doi: 10.1053/j.gastro.2012.09.002.

[41] A. Lombardi, A. Grimaldi, S. Zappavigna, G. Misso, and M. Caraglia, "Hepatocarcinoma: genetic and epigenetic features," *Minerva Gastroenterol Dietol,* vol. 64, no. 1, pp. 14-27, Mar 2018, doi: 10.23736/S1121-421X.17.02408-4.

[42] S. Boyault *et al.*, "Transcriptome classification of HCC is related to gene alterations and to new therapeutic targets," *Hepatology,* vol. 45, no. 1, pp. 42-52, Jan 2007, doi: 10.1002/hep.21467.

[43] D. Sia, A. Villanueva, S. L. Friedman, and J. M. Llovet, "Liver Cancer Cell of Origin, Molecular Class, and Effects on Patient Prognosis," *Gastroenterology,* vol. 152, no. 4, pp. 745-761, Mar 2017, doi: 10.1053/j.gastro.2016.11.048.

[44] V. T. DeVita, Jr. and E. Chu, "A history of cancer chemotherapy," *Cancer Res,* vol. 68, no. 21, pp. 8643-53, Nov 1 2008, doi: 10.1158/0008-5472.CAN-07-6611.

[45] S. M. Biplob Bhattacharya, "Cancer Therapy Using Antibiotics," *Journal of Cancer Therapy,* vol. 6, pp. 849-858, 2015, doi: 10.4236/jct.2015.610093

[46] F. Zunino and G. Capranico, "DNA topoisomerase II as the primary target of anti-tumor anthracyclines," *Anticancer Drug Des,* vol. 5, no. 4, pp. 307-17, Nov 1990. [Online]. Available: https://www.ncbi.nlm.nih.gov/pubmed/1963303.

[47] Q. Sun *et al.*, "MUTYH Deficiency Is Associated with Attenuated Pulmonary Fibrosis in a Bleomycin-Induced Model," *Oxid Med Cell Longev,* vol. 2020, p. 4828256, 2020, doi: 10.1155/2020/4828256.

[48] N. Miyagawa, D. Sasaki, M. Matsuoka, M. Imanishi, T. Ando, and Y. Sugiura, "DNA cleavage characteristics of non-protein enediyne antibiotic N1999A2," *Biochem Biophys Res Commun,* vol. 306, no. 1, pp. 87-92, Jun 20 2003, doi: 10.1016/s0006-291x(03)00925-2.

[49] D. A. Kevin Ii, D. A. Meujo, and M. T. Hamann, "Polyether ionophores: broad-spectrum and promising biologically active molecules for the control of drug-resistant bacteria and parasites," *Expert Opin Drug Discov,* vol. 4, no. 2, pp. 109-46, Feb 2009, doi: 10.1517/17460440802661443.

[50] M. Antoszczak, "A medicinal chemistry perspective on salinomycin as a potent anticancer and anti-CSCs agent," *Eur J Med Chem,* vol. 164, pp. 366-377, Feb 15 2019, doi: 10.1016/j.ejmech.2018.12.057.

[51] D. Qi, Y. Liu, J. Li, J. H. Huang, X. Hu, and E. Wu, "Salinomycin as a potent anticancer stem cell agent: State of the art and future directions," *Med Res Rev,* Nov 16 2021, doi: 10.1002/med.21870.

[52] M. Sulik, E. Maj, J. Wietrzyk, A. Huczynski, and M. Antoszczak, "Synthesis and Anticancer Activity of Dimeric Polyether Ionophores," *Biomolecules,* vol. 10, no. 7, Jul 12 2020, doi: 10.3390/biom10071039.

[53] J. Dewangan, S. Srivastava, and S. K. Rath, "Salinomycin: A new paradigm in cancer therapy," *Tumour Biol,* vol. 39, no. 3, p. 1010428317695035, Mar 2017, doi: 10.1177/1010428317695035.

[54] P. B. Gupta *et al.*, "Identification of selective inhibitors of cancer stem cells by high-throughput screening," *Cell,* vol. 138, no. 4, pp. 645-659, Aug 21 2009, doi: 10.1016/j.cell.2009.06.034.

[55] D. Lu, M. Y. Choi, J. Yu, J. E. Castro, T. J. Kipps, and D. A. Carson, "Salinomycin inhibits Wnt signaling and selectively induces apoptosis in chronic lymphocytic leukemia cells," *Proc Natl Acad Sci U S A,* vol. 108, no. 32, pp. 13253-7, Aug 9 2011, doi: 10.1073/pnas.1110431108.

[56] D. S. Wishart *et al.*, "DrugBank 5.0: a major update to the DrugBank database for 2018," *Nucleic Acids Res,* vol. 46, no. D1, pp. D1074-D1082, Jan 4 2018, doi: 10.1093/nar/gkx1037.

[57] S. R. Mathachan, K. Sardana, and A. Khurana, "Current Use of Ivermectin in Dermatology, Tropical Medicine, and COVID-19: An Update on Pharmacology, Uses, Proven and Varied Proposed Mechanistic Action," *Indian Dermatol Online J,* vol. 12, no. 4, pp. 500-514, Jul-Aug 2021, doi: 10.4103/idoj.idoj_298_21.

[58] G. Dominguez-Gomez *et al.*, "Ivermectin as an inhibitor of cancer stemlike cells," *Mol Med Rep,* vol. 17, no. 2, pp. 3397-3403, Feb 2018, doi: 10.3892/mmr.2017.8231.

[59] M. Juarez, A. Schcolnik-Cabrera, and A. Duenas-Gonzalez, "The multitargeted drug ivermectin: from an antiparasitic agent to a repositioned cancer drug," *Am J Cancer Res,* vol. 8, no. 2, pp. 317-331, 2018. [Online]. Available: https://www.ncbi.nlm.nih.gov/pubmed/29511601.

[60] A. Melotti, C. Mas, M. Kuciak, A. Lorente-Trigos, I. Borges, and A. Ruiz i Altaba, "The river blindness drug Ivermectin and related macrocyclic lactones inhibit WNT-TCF pathway responses in human cancer," *EMBO Mol Med,* vol. 6, no. 10, pp. 1263-78, Oct 2014, doi: 10.15252/emmm.201404084.

[61] S. Nambara *et al.*, "Antitumor effects of the antiparasitic agent ivermectin via inhibition of Yes-associated protein 1 expression in gastric cancer," *Oncotarget,* vol. 8, no. 64, pp. 107666-107677, Dec 8 2017, doi: 10.18632/oncotarget.22587.

[62] Q. Dou *et al.*, "Ivermectin Induces Cytostatic Autophagy by Blocking the PAK1/Akt Axis in Breast Cancer," *Cancer Res,* vol. 76, no. 15, pp. 4457-69, Aug 1 2016, doi: 10.1158/0008-5472.CAN-15-2887.

[63] M. Antoszczak, D. Steverding, and A. Huczynski, "Anti-parasitic activity of polyether ionophores," *Eur J Med Chem,* vol. 166, pp. 32-47, Mar 15 2019, doi: 10.1016/j.ejmech.2019.01.035.

[64] H. D. Chapman, T. K. Jeffers, and R. B. Williams, "Forty years of monensin for the control of coccidiosis in poultry," *Poult Sci,* vol. 89, no. 9, pp. 1788-801, Sep 2010, doi: 10.3382/ps.2010-00931.

[65] W. H. Park *et al.*, "Monensin inhibits the growth of renal cell carcinoma cells via cell cycle arrest or apoptosis," *Int J Oncol,* vol. 22, no. 4, pp. 855-60, Apr 2003. [Online]. Available: https://www.ncbi.nlm.nih.gov/pubmed/12632079.

[66] W. H. Park, E. S. Kim, C. W. Jung, B. K. Kim, and Y. Y. Lee, "Monensin-mediated growth inhibition of SNU-C1 colon cancer cells via cell cycle arrest and apoptosis," *Int J Oncol,* vol. 22, no. 2, pp. 377-82, Feb 2003. [Online]. Available: https://www.ncbi.nlm.nih.gov/pubmed/12527937.

[67] W. H. Park, E. S. Kim, B. K. Kim, and Y. Y. Lee, "Monensin-mediated growth inhibition in NCI-H929 myeloma cells via cell cycle arrest and apoptosis," *Int J Oncol,* vol. 23, no. 1, pp. 197-204, Jul 2003. [Online]. Available: https://www.ncbi.nlm.nih.gov/pubmed/12792794.

[68] W. H. Park, M. S. Lee, K. Park, E. S. Kim, B. K. Kim, and Y. Y. Lee, "Monensin-mediated growth inhibition in acute myelogenous leukemia cells via cell cycle arrest and apoptosis," *Int J Cancer,* vol. 101, no. 3, pp. 235-42, Sep 20 2002, doi: 10.1002/ijc.10592.

[69] Y. Deng *et al.*, "Antibiotic monensin synergizes with EGFR inhibitors and oxaliplatin to suppress the proliferation of human ovarian cancer cells," *Sci Rep,* vol. 5, p. 17523, Dec 7 2015, doi: 10.1038/srep17523.

[70] X. Wang *et al.*, "Monensin inhibits cell proliferation and tumor growth of chemo-resistant pancreatic cancer cells by targeting the EGFR signaling pathway," *Sci Rep,* vol. 8, no. 1, p. 17914, Dec 17 2018, doi: 10.1038/s41598-018-36214-5.

[71] K. Iljin *et al.*, "High-throughput cell-based screening of 4910 known drugs and drug-like small molecules identifies disulfiram as an inhibitor of prostate cancer cell growth," *Clin Cancer Res,* vol. 15, no. 19, pp. 6070-8, Oct 1 2009, doi: 10.1158/1078-0432.CCR-09-1035.

[72] M. Vanneste *et al.*, "High content screening identifies monensin as an EMT-selective cytotoxic compound," *Sci Rep,* vol. 9, no. 1, p. 1200, Feb 4 2019, doi: 10.1038/s41598-018-38019-y.

[73] W. E. Rose and M. J. Rybak, "Tigecycline: first of a new class of antimicrobial agents," *Pharmacotherapy,* vol. 26, no. 8, pp. 1099-110, Aug 2006, doi: 10.1592/phco.26.8.1099.

[74] N. Kasbekar, "Tigecycline: a new glycylcycline antimicrobial agent," *Am J Health Syst Pharm,* vol. 63, no. 13, pp. 1235-43, Jul 1 2006, doi: 10.2146/ajhp050487.

[75] C. M. Slover, K. A. Rodvold, and L. H. Danziger, "Tigecycline: a novel broad-spectrum antimicrobial," *Ann Pharmacother,* vol. 41, no. 6, pp. 965-72, Jun 2007, doi: 10.1345/aph.1H543.

[76] M. Skrtic *et al.*, "Inhibition of mitochondrial translation as a therapeutic strategy for human acute myeloid leukemia," *Cancer Cell,* vol. 20, no. 5, pp. 674-88, Nov 15 2011, doi: 10.1016/j.ccr.2011.10.015.

[77] C. Tang *et al.*, "Antibiotic drug tigecycline inhibited cell proliferation and induced autophagy in gastric cancer cells," *Biochem Biophys Res Commun,* vol. 446, no. 1, pp. 105-12, Mar 28 2014, doi: 10.1016/j.bbrc.2014.02.043.

[78] R. A. Jones *et al.*, "RB1 deficiency in triple-negative breast cancer induces mitochondrial protein translation," *J Clin Invest,* vol. 126, no. 10, pp. 3739-3757, Oct 3 2016, doi: 10.1172/JCI81568.

[79] H. Li, S. Jiao, X. Li, H. Banu, S. Hamal, and X. Wang, "Therapeutic effects of antibiotic drug tigecycline against cervical squamous cell carcinoma by inhibiting Wnt/beta-catenin signaling," *Biochem Biophys Res Commun,* vol. 467, no. 1, pp. 14-20, Nov 6 2015, doi: 10.1016/j.bbrc.2015.09.140.

[80] J. Tan, M. Song, M. Zhou, and Y. Hu, "Antibiotic tigecycline enhances cisplatin activity against human hepatocellular carcinoma through inducing mitochondrial dysfunction and oxidative damage," *Biochem Biophys Res Commun,* vol. 483, no. 1, pp. 17-23, Jan 29 2017, doi: 10.1016/j.bbrc.2017.01.021.

[81] X. Jia, Z. Gu, W. Chen, and J. Jiao, "Tigecycline targets nonsmall cell lung cancer through inhibition of mitochondrial function," *Fundam Clin Pharmacol,* vol. 30, no. 4, pp. 297-306, Aug 2016, doi: 10.1111/fcp.12199.

[82] A. Ren, Y. Qiu, H. Cui, and G. Fu, "Tigecycline exerts an antitumoral effect in oral squamous cell carcinoma," *Oral Dis,* vol. 21, no. 5, pp. 558-64, Jul 2015, doi: 10.1111/odi.12311.

[83] R. Yang *et al.*, "Tigecycline Inhibits Glioma Growth by Regulating miRNA-199b-5p-HES1-AKT Pathway," *Mol Cancer Ther,* vol. 15, no. 3, pp. 421-9, Mar 2016, doi: 10.1158/1535-7163.MCT-15-0709.

[84] X. Fu, W. Liu, Q. Huang, Y. Wang, H. Li, and Y. Xiong, "Targeting mitochondrial respiration selectively sensitizes pediatric acute lymphoblastic leukemia cell lines and patient samples to standard chemotherapy," *Am J Cancer Res,* vol. 7, no. 12, pp. 2395-2405, 2017. [Online]. Available: https://www.ncbi.nlm.nih.gov/pubmed/29312795.

[85] "Testing for neurological involvement in HIV infection," *Lancet,* vol. 2, no. 8574, pp. 1531-2, Dec 26 1987. [Online]. Available: https://www.ncbi.nlm.nih.gov/pubmed/2892095.

[86] B. Hu and Y. Guo, "Inhibition of mitochondrial translation as a therapeutic strategy for human ovarian cancer to overcome chemoresistance," *Biochem Biophys Res Commun,* vol. 509, no. 2, pp. 373-378, Feb 5 2019, doi: 10.1016/j.bbrc.2018.12.127.

[87] J. L. Koff, S. Ramachandiran, and L. Bernal-Mizrachi, "A time to kill: targeting apoptosis in cancer," *Int J Mol Sci,* vol. 16, no. 2, pp. 2942-55, Jan 28 2015, doi: 10.3390/ijms16022942.

[88] H. Hu *et al.*, "Antibiotic drug tigecycline inhibits melanoma progression and metastasis in a p21CIP1/Waf1-dependent manner," *Oncotarget,* vol. 7, no. 3, pp. 3171-85, Jan 19 2016, doi: 10.18632/oncotarget.6419.

[89] Z. Lu *et al.*, "Inhibition of autophagy enhances the selective anti-cancer activity of tigecycline to overcome drug resistance in the treatment of chronic myeloid leukemia," *J Exp Clin Cancer Res,* vol. 36, no. 1, p. 43, Mar 10 2017, doi: 10.1186/s13046-017-0512-6.

[90] R. K. Amaravadi, A. C. Kimmelman, and J. Debnath, "Targeting Autophagy in Cancer: Recent Advances and Future Directions," *Cancer Discov,* vol. 9, no. 9, pp. 1167-1181, Sep 2019, doi: 10.1158/2159-8290.CD-19-0292.

[91] Z. Dong and H. Cui, "The Autophagy-Lysosomal Pathways and Their Emerging Roles in Modulating Proteostasis in Tumors," *Cells,* vol. 8, no. 1, Dec 20 2018, doi: 10.3390/cells8010004.

[92] R. Ma *et al.*, "Inhibition of autophagy enhances the antitumour activity of tigecycline in multiple myeloma," *J Cell Mol Med,* vol. 22, no. 12, pp. 5955-5963, Dec 2018, doi: 10.1111/jcmm.13865.

[93] J. Yan *et al.*, "Carbon ion combined with tigecycline inhibits lung cancer cell proliferation by inducing mitochondrial dysfunction," *Life Sci,* vol. 263, p. 118586, Dec 15 2020, doi: 10.1016/j.lfs.2020.118586.

[94] X. Zhong *et al.*, "Antibiotic drug tigecycline reduces neuroblastoma cells proliferation by inhibiting Akt activation in vitro and in vivo," *Tumour Biol,* vol. 37, no. 6, pp. 7615-23, Jun 2016, doi: 10.1007/s13277-015-4613-6.

[95] Y. Xiong *et al.*, "Tigecycline as a dual inhibitor of retinoblastoma and angiogenesis via inducing mitochondrial dysfunctions and oxidative damage," *Sci Rep,* vol. 8, no. 1, p. 11747, Aug 6 2018, doi: 10.1038/s41598-018-29938-x.

[96] A. Acevedo and C. Gonzalez-Billault, "Crosstalk between Rac1-mediated actin regulation and ROS production," *Free Radic Biol Med,* vol. 116, pp. 101-113, Feb 20 2018, doi: 10.1016/j.freeradbiomed.2018.01.008.

[97] G. M. Cooper, "The Eukaryotic Cell Cycle," in *The Cell: A Molecular Approach.*, 2000, ch. The Eukaryotic Cell Cycle.

[98] Y. Wang *et al.*, "The double-edged roles of ROS in cancer prevention and therapy," *Theranostics,* vol. 11, no. 10, pp. 4839-4857, 2021, doi: 10.7150/thno.56747.

[99] E. Calvo *et al.*, "Everolimus in metastatic renal cell carcinoma: Subgroup analysis of patients with 1 or 2 previous vascular endothelial growth factor receptor-tyrosine kinase inhibitor therapies enrolled in the phase III RECORD-1 study," *Eur J Cancer,* vol. 48, no. 3, pp. 333-9, Feb 2012, doi: 10.1016/j.ejca.2011.11.027.

[100] S. E. Grigg, G. L. Sarri, P. J. Gow, and N. D. Yeomans, "Systematic review with meta-analysis: sirolimus- or everolimus-based immunosuppression following liver transplantation for hepatocellular carcinoma," *Aliment Pharmacol Ther,* vol. 49, no. 10, pp. 1260-1273, May 2019, doi: 10.1111/apt.15253.

[101] M. Guba *et al.*, "Rapamycin inhibits primary and metastatic tumor growth by antiangiogenesis: involvement of vascular endothelial growth factor," *Nat Med,* vol. 8, no. 2, pp. 128-35, Feb 2002, doi: 10.1038/nm0202-128.

[102] M. Messner *et al.*, "Metabolic implication of tigecycline as an efficacious second-line treatment for sorafenib-resistant hepatocellular carcinoma," *FASEB J,* vol. 34, no. 9, pp. 11860-11882, Sep 2020, doi: 10.1096/fj.202001128R.

[103] J. Shi, X. Wang, L. Lyu, H. Jiang, and H. J. Zhu, "Comparison of protein expression between human livers and the hepatic cell lines HepG2, Hep3B, and Huh7 using SWATH and MRM-HR proteomics: Focusing on drug-metabolizing enzymes," *Drug Metab Pharmacokinet,* vol. 33, no. 2, pp. 133-140, Apr 2018, doi: 10.1016/j.dmpk.2018.03.003.

[104] B. B. Knowles, C. C. Howe, and D. P. Aden, "Human hepatocellular carcinoma cell lines secrete the major plasma proteins and hepatitis B surface antigen," *Science,* vol. 209, no. 4455, pp. 497-9, Jul 25 1980, doi: 10.1126/science.6248960.

[105] H. Nakabayashi, K. Taketa, K. Miyano, T. Yamane, and J. Sato, "Growth of human hepatoma cells lines with differentiated functions in chemically defined medium," *Cancer Res,* vol. 42, no. 9, pp. 3858-63, Sep 1982. [Online]. Available: https://www.ncbi.nlm.nih.gov/pubmed/6286115.

[106] D. P. Aden, A. Fogel, S. Plotkin, I. Damjanov, and B. B. Knowles, "Controlled synthesis of HBsAg in a differentiated human liver carcinoma-derived cell line," *Nature,* vol. 282, no. 5739, pp. 615-6, Dec 6 1979, doi: 10.1038/282615a0.

[107] S. Sell and H. L. Leffert, "Liver cancer stem cells," *J Clin Oncol,* vol. 26, no. 17, pp. 2800-5, Jun 10 2008, doi: 10.1200/JCO.2007.15.5945.

[108] I. K. Olivares-Marin, J. C. Gonzalez-Hernandez, and L. A. Madrigal-Perez, "Resveratrol cytotoxicity is energy-dependent," *J Food Biochem,* vol. 43, no. 9, p. e13008, Sep 2019, doi: 10.1111/jfbc.13008.

[109] A. B. Jaffe and A. Hall, "Rho GTPases: biochemistry and biology," *Annu Rev Cell Dev Biol,* vol. 21, pp. 247-69, 2005, doi: 10.1146/annurev.cellbio.21.020604.150721.

[110] E. Pedersen and C. Brakebusch, "Rho GTPase function in development: how in vivo models change our view," *Exp Cell Res,* vol. 318, no. 14, pp. 1779-87, Aug 15 2012, doi: 10.1016/j.yexcr.2012.05.004.

[111] G. C. Prendergast, R. Khosravi-Far, P. A. Solski, H. Kurzawa, P. F. Lebowitz, and C. J. Der, "Critical role of Rho in cell transformation by oncogenic Ras," *Oncogene,* vol. 10, no. 12, pp. 2289-96, Jun 15 1995. [Online]. Available: https://www.ncbi.nlm.nih.gov/pubmed/7784077.

[112] E. Hodis *et al.*, "A landscape of driver mutations in melanoma," *Cell,* vol. 150, no. 2, pp. 251-63, Jul 20 2012, doi: 10.1016/j.cell.2012.06.024.

[113] M. Krauthammer *et al.*, "Exome sequencing identifies recurrent somatic RAC1 mutations in melanoma," *Nat Genet,* vol. 44, no. 9, pp. 1006-14, Sep 2012, doi: 10.1038/ng.2359.

[114] J. L. Kissil *et al.*, "Requirement for Rac1 in a K-ras induced lung cancer in the mouse," *Cancer Res,* vol. 67, no. 17, pp. 8089-94, Sep 1 2007, doi: 10.1158/0008-5472.CAN-07-2300.

[115] C. Y. Wu *et al.*, "PI3K regulation of RAC1 is required for KRAS-induced pancreatic tumorigenesis in mice," *Gastroenterology,* vol. 147, no. 6, pp. 1405-16 e7, Dec 2014, doi: 10.1053/j.gastro.2014.08.032.

[116] P. De, J. C. Aske, and N. Dey, "RAC1 Takes the Lead in Solid Tumors," *Cells,* vol. 8, no. 5, Apr 26 2019, doi: 10.3390/cells8050382.

[117] M. Yamaguchi *et al.*, "Rac1 activation in human breast carcinoma as a prognostic factor associated with therapeutic resistance," *Breast Cancer,* vol. 27, no. 5, pp. 919-928, Sep 2020, doi: 10.1007/s12282-020-01091-2.

[118] G. A. Cardama *et al.*, "Relevance of small GTPase Rac1 pathway in drug and radio-resistance mechanisms: Opportunities in cancer therapeutics," *Crit Rev Oncol Hematol,* vol. 124, pp. 29-36, Apr 2018, doi: 10.1016/j.critrevonc.2018.01.012.

[119] A. Abo, E. Pick, A. Hall, N. Totty, C. G. Teahan, and A. W. Segal, "Activation of the NADPH oxidase involves the small GTP-binding protein p21rac1," *Nature,* vol. 353, no. 6345, pp. 668-70, Oct 17 1991, doi: 10.1038/353668a0.

[120] R. D. Fritz and O. Pertz, "The dynamics of spatio-temporal Rho GTPase signaling: formation of signaling patterns," *F1000Res,* vol. 5, 2016, doi: 10.12688/f1000research.7370.1.

[121] S. J. Hanna *et al.*, "The Role of Rho-GTPases and actin polymerization during Macrophage Tunneling Nanotube Biogenesis," *Sci Rep,* vol. 7, no. 1, p. 8547, Aug 17 2017, doi: 10.1038/s41598-017-08950-7.

[122] A. Woroniuk *et al.*, "STEF/TIAM2-mediated Rac1 activity at the nuclear envelope regulates the perinuclear actin cap," *Nat Commun,* vol. 9, no. 1, p. 2124, May 29 2018, doi: 10.1038/s41467-018-04404-4.

[123] D. Michaelson *et al.*, "Rac1 accumulates in the nucleus during the G2 phase of the cell cycle and promotes cell division," *J Cell Biol,* vol. 181, no. 3, pp. 485-96, May 5 2008, doi: 10.1083/jcb.200801047.

[124] M. May, I. Schelle, C. Brakebusch, K. Rottner, and H. Genth, "Rac1-dependent recruitment of PAK2 to G2 phase centrosomes and their roles in the regulation of mitotic entry," *Cell Cycle,* vol. 13, no. 14, pp. 2211-21, 2014, doi: 10.4161/cc.29279.

[125] Z. Diamantopoulou *et al.*, "TIAM1 Antagonizes TAZ/YAP Both in the Destruction Complex in the Cytoplasm and in the Nucleus to Inhibit Invasion of Intestinal Epithelial Cells," *Cancer Cell,* vol. 31, no. 5, pp. 621-634 e6, May 8 2017, doi: 10.1016/j.ccell.2017.03.007.

[126] Y. Shi *et al.*, "Rac1-Mediated DNA Damage and Inflammation Promote Nf2 Tumorigenesis but Also Limit Cell-Cycle Progression," *Dev Cell,* vol. 39, no. 4, pp. 452-465, Nov 21 2016, doi: 10.1016/j.devcel.2016.09.027.

[127] R. Velaithan *et al.*, "The small GTPase Rac1 is a novel binding partner of Bcl-2 and stabilizes its antiapoptotic activity," *Blood,* vol. 117, no. 23, pp. 6214-26, Jun 9 2011, doi: 10.1182/blood-2010-08-301283.

[128] Y. Pan, N. Wang, P. Xia, E. Wang, Q. Guo, and Z. Ye, "Inhibition of Rac1 ameliorates neuronal oxidative stress damage via reducing Bcl-2/Rac1 complex formation in mitochondria through PI3K/Akt/mTOR pathway," *Exp Neurol,* vol. 300, pp. 149-166, Feb 2018, doi: 10.1016/j.expneurol.2017.10.030.

[129] R. A. Kowluru *et al.*, "TIAM1-RAC1 signalling axis-mediated activation of NADPH oxidase-2 initiates mitochondrial damage in the development of diabetic retinopathy," *Diabetologia,* vol. 57, no. 5, pp. 1047-56, May 2014, doi: 10.1007/s00125-014-3194-z.

[130] H. L. Osborn-Heaford *et al.*, "Mitochondrial Rac1 GTPase import and electron transfer from cytochrome c are required for pulmonary fibrosis," *J Biol Chem,* vol. 287, no. 5, pp. 3301-12, Jan 27 2012, doi: 10.1074/jbc.M111.308387.

[131] Z. B. Jiang *et al.*, "miR-365 regulates liver cancer stem cells via RAC1 pathway," *Mol Carcinog,* vol. 58, no. 1, pp. 55-65, Jan 2019, doi: 10.1002/mc.22906.

[132] R. Z. Ran *et al.*, "miR-194 inhibits liver cancer stem cell expansion by regulating RAC1 pathway," *Exp Cell Res,* vol. 378, no. 1, pp. 66-75, May 1 2019, doi: 10.1016/j.yexcr.2019.03.007.

[133] A. de Conti *et al.*, "Butyrate-containing structured lipids inhibit RAC1 and epithelial-to-mesenchymal transition markers: a chemopreventive mechanism against hepatocarcinogenesis," *J Nutr Biochem,* vol. 86, p. 108496, Dec 2020, doi: 10.1016/j.jnutbio.2020.108496.

[134] Y. Li *et al.*, "Overexpression of Opa interacting protein 5 increases the progression of liver cancer via BMPR2/JUN/CHEK1/RAC1 dysregulation," *Oncol Rep,* vol. 41, no. 4, pp. 2075-2088, Apr 2019, doi: 10.3892/or.2019.7006.

[135] A. Payapilly and A. Malliri, "Compartmentalisation of RAC1 signalling," *Curr Opin Cell Biol,* vol. 54, pp. 50-56, Oct 2018, doi: 10.1016/j.ceb.2018.04.009.

[136] Y. Zhou *et al.*, "YAP promotes multi-drug resistance and inhibits autophagy-related cell death in hepatocellular carcinoma via the RAC1-ROS-mTOR pathway," *Cancer Cell Int,* vol. 19, p. 179, 2019, doi: 10.1186/s12935-019-0898-7.

[137] E. C. Cheung *et al.*, "Opposing effects of TIGAR- and RAC1-derived ROS on Wnt-driven proliferation in the mouse intestine," *Genes Dev,* vol. 30, no. 1, pp. 52-63, Jan 1 2016, doi: 10.1101/gad.271130.115.

[138] D. Kirmani, H. F. Bhat, M. Bashir, M. A. Zargar, and F. A. Khanday, "P66Shc-rac1 pathway-mediated ROS production and cell migration is downregulated by ascorbic acid," *J Recept Signal Transduct Res,* vol. 33, no. 2, pp. 107-13, Apr 2013, doi: 10.3109/10799893.2013.770527.

[139] W. Xie, W. Zhang, M. Sun, C. Lu, and Y. Shen, "Deacetylmycoepoxydiene is an agonist of Rac1, and simultaneously induces autophagy and apoptosis," *Appl Microbiol Biotechnol,* vol. 102, no. 14, pp. 5965-5975, Jul 2018, doi: 10.1007/s00253-018-9058-6.

[140] C. F. Mo *et al.*, "IQGAP1 promotes anoikis resistance and metastasis through Rac1-dependent ROS accumulation and activation of Src/FAK signalling in hepatocellular carcinoma," *Br J Cancer,* vol. 123, no. 7, pp. 1154-1163, Sep 2020, doi: 10.1038/s41416-020-0970-z.

[141] C. E. Tolbert, M. V. Beck, C. E. Kilmer, and M. C. Srougi, "Loss of ATM positively regulates Rac1 activity and cellular migration through oxidative stress," *Biochem Biophys Res Commun,* vol. 508, no. 4, pp. 1155-1161, Jan 22 2019, doi: 10.1016/j.bbrc.2018.12.033.

[142] X. Zhong, Y. Zhu, Y. Wang, Q. Zhao, and H. Huang, "Effects of three antibiotics on growth and antioxidant response of Chlorella pyrenoidosa and Anabaena cylindrica," *Ecotoxicol Environ Saf,* vol. 211, p. 111954, Mar 15 2021, doi: 10.1016/j.ecoenv.2021.111954.

[143] Y. Xiao, T. Xiong, X. Meng, D. Yu, Z. Xiao, and L. Song, "Different influences on mitochondrial function, oxidative stress and cytotoxicity of antibiotics on primary human neuron and cell lines," *J Biochem Mol Toxicol,* vol. 33, no. 4, p. e22277, Apr 2019, doi: 10.1002/jbt.22277.

[144] D. Nolfi-Donegan, A. Braganza, and S. Shiva, "Mitochondrial electron transport chain: Oxidative phosphorylation, oxidant production, and methods of measurement," *Redox Biol,* vol. 37, p. 101674, Oct 2020, doi: 10.1016/j.redox.2020.101674.

[145] K. Vermeulen, D. R. Van Bockstaele, and Z. N. Berneman, "The cell cycle: a review of regulation, deregulation and therapeutic targets in cancer," *Cell Prolif,* vol. 36, no. 3, pp. 131-49, Jun 2003, doi: 10.1046/j.1365-2184.2003.00266.x.

[146] T. Otto and P. Sicinski, "Cell cycle proteins as promising targets in cancer therapy," *Nat Rev Cancer,* vol. 17, no. 2, pp. 93-115, Jan 27 2017, doi: 10.1038/nrc.2016.138.

[147] J. Yang *et al.*, "Antibiotic tigecycline inhibits cell proliferation, migration and invasion via down-regulating CCNE2 in pancreatic ductal adenocarcinoma," *J Cell Mol Med,* vol. 24, no. 7, pp. 4245-4260, Apr 2020, doi: 10.1111/jcmm.15086.

[148] J. Van't Hof, "Control of cell progression through the mitotic cycle by carbohydrate provision. I. Regulation of cell division in excised plant tissue," *J Cell Biol,* vol. 37, no. 3, pp. 773-80, Jun 1968, doi: 10.1083/jcb.37.3.773.

[149] E. Robbins and G. A. Morrill, "Oxygen uptake during the HeLa cell life cycle and its correlation with macromolecular synthesis," *J Cell Biol,* vol. 43, no. 3, pp. 629-33, Dec 1969, doi: 10.1083/jcb.43.3.629.

[150] T. Wang, C. Marquardt, and J. Foker, "Aerobic glycolysis during lymphocyte proliferation," *Nature,* vol. 261, no. 5562, pp. 702-5, Jun 24 1976, doi: 10.1038/261702a0.

[151] M. Salazar-Roa and M. Malumbres, "Fueling the Cell Division Cycle," *Trends Cell Biol,* vol. 27, no. 1, pp. 69-81, Jan 2017, doi: 10.1016/j.tcb.2016.08.009.

[152] G. Housman *et al.*, "Drug resistance in cancer: an overview," *Cancers (Basel),* vol. 6, no. 3, pp. 1769-92, Sep 5 2014, doi: 10.3390/cancers6031769.

[153] B. Wang, J. Ao, D. Yu, T. Rao, Y. Ruan, and X. Yao, "Inhibition of mitochondrial translation effectively sensitizes renal cell carcinoma to chemotherapy," *Biochem Biophys Res Commun,* vol. 490, no. 3, pp. 767-773, Aug 26 2017, doi: 10.1016/j.bbrc.2017.06.115.

[154] A. D'Andrea *et al.*, "The mitochondrial translation machinery as a therapeutic target in Myc-driven lymphomas," *Oncotarget,* vol. 7, no. 45, pp. 72415-72430, Nov 8 2016, doi: 10.18632/oncotarget.11719.

[155] M. Rava *et al.*, "Therapeutic synergy between tigecycline and venetoclax in a preclinical model of MYC/BCL2 double-hit B cell lymphoma," *Sci Transl Med,* vol. 10, no. 426, Jan 31 2018, doi: 10.1126/scitranslmed.aan8723.

[156] B. Escudier *et al.*, "CheckMate 025 Randomized Phase 3 Study: Outcomes by Key Baseline Factors and Prior Therapy for Nivolumab Versus Everolimus in Advanced Renal Cell Carcinoma," *Eur Urol,* vol. 72, no. 6, pp. 962-971, Dec 2017, doi: 10.1016/j.eururo.2017.02.010.

[157] J. Baselga *et al.*, "Everolimus in postmenopausal hormone-receptor-positive advanced breast cancer," *N Engl J Med,* vol. 366, no. 6, pp. 520-9, Feb 9 2012, doi: 10.1056/NEJMoa1109653.

[158] L. B. Jeng *et al.*, "Experience of using everolimus in the early stage of living donor liver transplantation," *Transplant Proc,* vol. 46, no. 3, pp. 744-8, Apr 2014, doi: 10.1016/j.transproceed.2013.11.068.

[159] T. K. Burki, "Poor results for everolimus in patients with liver cancer," *Lancet Oncol,* vol. 15, no. 9, p. e368, Aug 2014, doi: 10.1016/s1470-2045(14)70318-3.

Acknowledgements

More than two years of research will come to an end with the end of my project. Looking back on this short but long period, there are many people to thank. First of all, I would like to thank my supervisor, Prof. Dr. Alexandr Bazhin, who allowed me to carry out my research at the Ludwig-Maximilians University. I still remember that winter morning at 11:00 a.m. when he had a friendly conversation with me in the hospital hall and allowed me to study and research in his laboratory. It was very important to me at that time, like a hand reaching out from heaven to bring me out of hell. I have made no secret of my gratitude and respect for him. He was also someone who helped me a lot with my project, first of all, because he had a good scientific mind and knew a lot of research methodsand was always there to help me when I was in trouble.

Next， I would like to thank my direct supervisor, Dr. med. Dominik Koch. He has been a very reliable research partner and we have had in-depth conversations on the subject. He has always given me a lot of support and made me brave enough to explore. He is also a great friend and has helped me in many ways. In particular, he provided great help with the revision of articles. He has also been a great help to me in many of my administrative processes. I hope I can maintain a lifelong friendship with him.

Thank you to PD Dr. med. Matthias Ilmer and PD Dr. med. Bernhard Renz who met with us every Thursday for lab meetings. They are both fantastic doctors and scientists. They have given us a lot of valuable advice on topics and experiments in progress. I am also grateful for their financial support.

My sincere thanks to Ms. Natalja Ring, Ms. Mudusetti Shristee and Ms. Issar Amerchel, Sevdije. I thank them for the technical support they provided. Also, cherish the happy times we had to work together in the lab. They are also the ones who made my life in Germany more colorful.

Thanks to all my colleagues in the Klinik für Allgemein-, Viszeral- und Transplantationschirurgie in our lab.

Thanks to the scholarship support from the China Scholarship Council, I was able to complete my project without any worries.

Last but not least, I would like to thank my family and friends, especially Ms Xin Yue, who have always encouraged me and supported me. Without their help, I would not have been able to complete this research.

Affidavit

LMU LUDWIG-MAXIMILIANS-UNIVERSITÄT MÜNCHEN

Promotionsbüro
Medizinische Fakultät

MMRS

Affidavit

Yu, Haochen
Surname, first name

Guardinistr 139,
Street

81375, Munich, Germany
Zip code, town, country

I hereby declare, that the submitted thesis entitled:

Tigecycline affects RAC1 and OXPHOS and shows antitumor effect in hepatocellular carcinoma

is my own work. I have only used the sources indicated and have not made unauthorised use of services of a third party. Where the work of others has been quoted or reproduced, the source is always given.
I further declare that the submitted thesis or parts thereof have not been presented as part of an examination degree to any other university.

Munich, 22.07.2022 — **Haochen Yu**

place, date — Signature doctoral candidate